

Modeling and performance analysis of OAM-GSM millimeter-wave wireless communication systems^{*}

Qi ZHANG, Xusheng XIONG, Qiang LI[‡], Tao HAN, Yi ZHONG

School of Electronic Information and Communication, Huazhong University of Science and Technology, Wuhan 430074, China

E-mail: qiqiz@hust.edu.cn; xiongxusheng@hust.edu.cn; qli_patrick@hust.edu.cn; hantao@hust.edu.cn; yzhong@hust.edu.cn

Received Aug. 31, 2020; Revision accepted Feb. 6, 2021; Crosschecked Mar. 15, 2021

Abstract: In recent years, the conventional degrees of freedom in frequency and time have been fully used. It is difficult to further improve the performance of communication systems with such degrees of freedom. Orbital angular momentum (OAM), which provides a new degree of freedom for millimeter-wave (mmWave) wireless communication systems, has been recognized as a key enabling technique for future mobile communication networks. By combining OAM beams that have theoretically infinite and mutually orthogonal states with the generalized spatial modulation (GSM) strategy, a new OAM-GSM mmWave wireless communication system is designed in this paper. A bit error rate (BER) model of the OAM-GSM system is established based on channel flip precoding. The channel capacity, energy efficiency, and BER of the proposed OAM-GSM mmWave wireless communication system are simulated. Numerical results show that, compared with traditional GSM systems, the OAM-GSM system has more complex transmission and reception mechanisms but the channel capacity and maximum achievable energy efficiency are increased by 80% and 54%, respectively, and the BER drops by 91.5%.

Key words: Orbital angular momentum (OAM); Generalized spatial modulation (GSM); Millimeter-wave communication; Channel capacity; Energy efficiency; Bit error rate (BER)

<https://doi.org/10.1631/FITEE.2000444>

CLC number: TN928

1 Introduction

In recent years, with the widespread use of mobile phones and other electronic products, the requirements for communication systems have gradually changed. The communication system needs to accommodate more users and a larger amount of data, and to meet higher quality-of-service (QoS) requirements. Correspondingly, the wireless communication industry has shown explosive growth (Rap-

port, 1996; GSMR, 2011). In traditional wireless communication systems such as multi-input multi-output (MIMO) (Goldsmith et al., 2003), modulation strategies such as spatial modulation (SM) (Mesleh et al., 2006) and generalized spatial modulation (GSM) (Younis et al., 2010) have been proposed to increase the transmission rate of millimeter-wave (mmWave) communication systems. At the same time, the conventional degrees of freedom in frequency and time have been fully used. It is difficult to further improve the performance of communication systems with the degrees of freedom mentioned above. Orbital angular momentum (OAM) technology can provide a new degree of freedom for wireless communication systems because of the theoretically infinite OAM states and natural orthogonality among different OAM states. With the increasing frequency of electromagnetic waves used in wireless communication systems, OAM technology has received much attention.

[‡] Corresponding author

^{*} Project supported by the National Natural Science Foundation of China (No. U2001210)

 ORCID: Qi ZHANG, <https://orcid.org/0000-0002-7486-7243>; Xusheng XIONG, <https://orcid.org/0000-0003-2457-6795>; Qiang LI, <https://orcid.org/0000-0003-1471-3821>; Tao HAN, <https://orcid.org/0000-0002-0782-7807>; Yi ZHONG, <https://orcid.org/0000-0001-5584-0988>

© Zhejiang University Press 2021

According to the classical electromagnetic field theory, electromagnetic waves have not only linear but also angular momentum (Beth, 1936). The angular momentum is divided into two parts. One is spin angular momentum (SAM) and the other is OAM. SAM is used mainly to describe the polarization state of electromagnetic waves, including two orthogonal states of vertical and horizontal polarization (Yao and Padgett, 2011). Unlike SAM with only two polarization states, OAM has multiple states (Yao and Padgett, 2011), and electromagnetic waves with different OAM states are orthogonal to each other. The primary characteristic of OAM beams is that their equiphase surfaces are curved ones that spiral along with the transmission of the electromagnetic beams. In addition, the OAM beam propagates in the form of a divergent circular ring, whose energy is concentrated mainly on the ring around the launch axis, namely the ring area of the OAM beam. In general, the radius of the ring increases with the increase of the transmission distance.

Allen L et al. (1992) discovered that Laguerre-Gaussian (LG) beams with helical phase wavefronts of azimuth $\exp(-j\ell\varphi)$ carry OAM, and proved that there exist an infinite number of discrete orthogonal OAM states for LG beams. Since then, OAM has been extensively studied in the field of optical communications. Gibson et al. (2004) encoded information on OAM states and demonstrated optical link communications based on OAM modulation in free space by experiment, and proved the unique confidentiality advantage of OAM communications. Wang J et al. combined OAM with traditional analog-division multiplexing technology (Wang J et al., 2012; Willner et al., 2012). The obtained free space optical communication system achieves a communication capacity of 2.56 Tb/s and a spectrum efficiency of 95.7 bits/(s·Hz).

The application of OAM has greatly improved the performance of optical communication systems, which inspires the application of OAM to the field of wireless communication. Thidé et al. (2007) used uniform circular arrays (UCAs) to generate OAM electromagnetic waves and proved that radio frequency electromagnetic waves also carry OAM states. In the experiment conducted in Venice, the authors used reflective spiral parabolic antennas to generate OAM signals and simultaneously transmitted two

signals in the same frequency band. The feasibility of OAM wireless transmission technology was verified for the first time and the use of OAM electromagnetic waves has the potential to greatly increase the wireless communication capacity (Tamburini et al., 2012). Schemmel et al. (2014) generated OAM beams in the mmWave band through spiral phase plates and measured the intensity and phase of OAM beam using three-dimensional (3D) detectors. A loop antenna theory was proposed (Hui et al., 2015; Zheng et al., 2015a, 2015b). Based on this theory, a slot antenna based on a ring cavity resonator was designed to simultaneously emit two or even four different OAM electromagnetic waves. In terms of OAM state detection, a phase gradient method was proposed (Mohammadi et al., 2010). In addition, compared with other traditional communication systems such as MIMO, whether or not the application of OAM waves can improve the channel capacity and spectrum efficiency of a communication system has been controversial in academic circles. Edfors and Johansson (2012) pointed out that the communication system using OAM states for information transmission is only a subset of MIMO systems and that the application of OAM waves cannot increase the capacity of communication systems. Scholars have used mmWave for communication and multiplexing the OAM state using the orthogonality among OAM states (Yan et al., 2014). A system with a transmission distance of 2.5 m was realized and the system finally achieved a spectral efficiency of 16 bits/(s·Hz). Zhang ZF et al. (2016) focused on the phase singularity of OAM beams and realized a new type of MIMO system combined with OAM technology. This confirmed that the channel capacity performance of MIMO systems combined with OAM technology is superior to that of traditional MIMO systems. Zhang WT et al. (2017) combined OAM electromagnetic waves with mode division multiplexing (MDM) technology to propose an OAM-MDM system, and their experiments proved that the OAM-MDM system has higher spectral efficiency and lower computational complexity than a traditional MIMO system. In addition, Allen B et al. (2014) put forward an idea of using the OAM state to encode and decode information bits. In addition, an OAM-SM system was proposed and a strategy for encoding and demodulation using the OAM state was given (Ge et al., 2017). In view of the

unique energy spatial distribution characteristics of OAM beams, Wang L et al. (2017) modeled OAM wireless communication channels. Simulations proved that the channel capacity of the OAM-MIMO system based on this channel model is superior to that of traditional MIMO systems.

The above-mentioned research on applying OAM to wireless communication systems focused mainly on the use of orthogonality between OAM states for channel multiplexing and performance comparisons with traditional MIMO systems. However, to the best of our knowledge, little research has used OAM states to encode and decode information. Although Allen B et al. (2014) proposed the idea of using OAM states to encode and decode information bits, no complete system was proposed. Although a complete system for coding and decoding information bits using the OAM state was proposed, it was limited to the combination of OAM and SM, in which an antenna is selected to be activated for signal transmission in a time slot (Ge et al., 2017). Inspired by the idea of using OAM states to encode signals, in this study OAM is combined with GSM, in which multiple antennas are activated for signal transmission in the same time slot. We study a signal detection algorithm of the OAM-GSM system, and model and simulate its channel capacity, energy efficiency, and bit error rate (BER). In addition, we optimize the BER performance using precoding algorithms. Simulations show that the OAM-GSM system can greatly increase the system capacity and maximum achievable energy

efficiency and reduce the system BER compared to traditional GSM systems. The main contributions of this article are as follows:

1. Combining OAM technology with GSM, a new type of multi-antenna mmWave wireless communication system is designed. This has potential for better performance.
2. The channel capacity, energy efficiency, and BER of the proposed OAM-GSM system are theoretically modeled and a channel flip precoding algorithm is used to improve the BER of the system.
3. Based on the modeling and performance analysis of channel capacity, energy efficiency, and BER of the OAM-GSM system, simulations show that significant performance gains can be achieved by the proposed OAM-GSM system as compared to traditional GSM systems.

2 OAM-GSM system model

2.1 OAM-GSM system model

The model diagram of the OAM-GSM system is shown in Fig. 1.

The distinguishing feature of a wireless OAM electromagnetic wave is that it has a helical phase wavefront, and the wavefront phase of a wireless OAM electromagnetic wave with different OAM states is also different. As such, the phase change of an OAM electromagnetic wave is sampled by two sampling antennas at the receiving end, based on

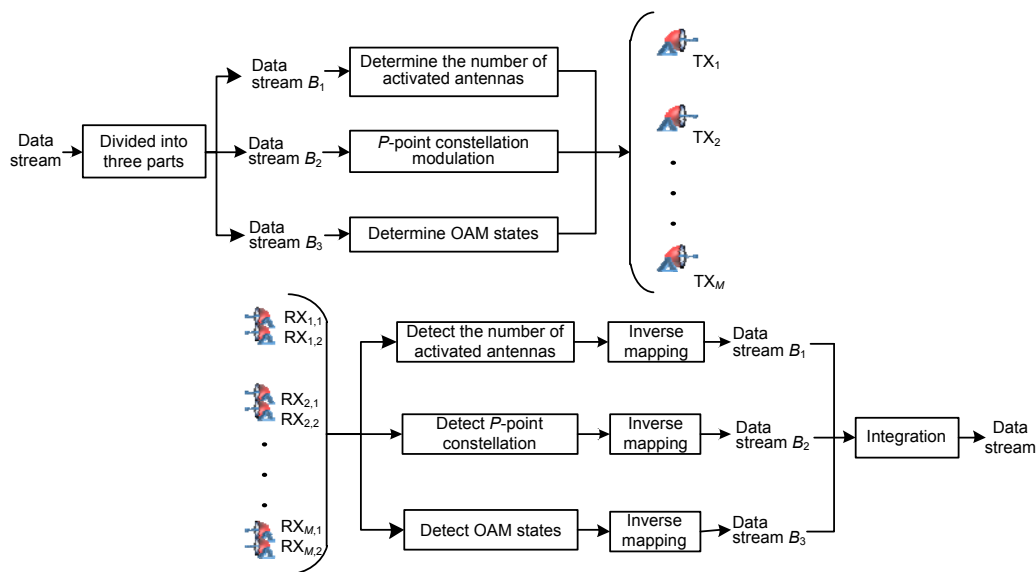


Fig. 1 System model of the proposed OAM-GSM mmWave communication system

which the OAM state of the OAM electromagnetic wave can be calculated using the phase gradient method. A uniform linear array composed of M OAM transmitting antennas is the transmitter of the OAM-GSM system. The receiver of the system consists of M groups of receiving antenna pairs, and each group of receiving antenna pairs contains two receiving antennas. The transmitter of the system uses the widely used Cassegrain antennas as OAM transmitting antennas (Zheng et al., 2015b). Cassegrain antennas can simultaneously generate multiple OAM waves with different OAM states; that is, a single antenna can be used to transmit electromagnetic waves in different OAM states and also switch OAM beams in different OAM states. By configuring a Cassegrain antenna with a reflector for beam focusing, the OAM beam emitted by it can be made more directional, so that the divergence angles of OAM

beams emitted in different OAM states are more similar. Therefore, at the same transmission distance, the ring areas of OAM beams in different OAM states have the same radius. In addition, the receiving antenna pairs at the receiver of the system are all arranged in the ring area of the OAM beam transmitted by the corresponding transmitting antenna. The main notations used in this paper are summarized in Table 1. In the system model of the OAM-GSM system, TX_n represents the n^{th} ($1 \leq n \leq M$) transmitting antenna at the transmitter. $RX_{m,1}$ and $RX_{m,2}$ represent the first and second antennas of the m^{th} ($1 \leq m \leq M$) receiving antenna pair at the receiver, respectively. The uniform linear array composed of the first antennas of M receiving antenna pairs at the receiver is placed in parallel with the uniform linear array at the transmitter. At the same time, the angle between the first and second antennas of all receiving antenna pairs is β .

Table 1 Simulation parameters

Symbol	Meaning	Symbol	Meaning
TX_n	The n^{th} transmitting antenna at the transmitter	\mathcal{Q}	OAM state set
$RX_{m,1}$	The first antenna of the m^{th} receiving antenna pair at the receiver	$d_{mn,1}$	Radial distance from receiving antenna $RX_{m,1}$ to transmitting antenna TX_n
$RX_{m,2}$	The second antenna of the m^{th} receiving antenna pair at the receiver	$d_{mn,2}$	Radial distance from receiving antenna $RX_{m,2}$ to transmitting antenna TX_n
β	The angle between the second antenna and the first antenna of all receiving antenna pairs	d_{nn}	Radial distance between transmitting antenna TX_n and receiving antenna $RX_{n,1}$
M	Number of transmitting antennas	$\theta_{mn,1}$	Azimuth of receiving antenna $RX_{m,1}$
M_a	Number of activated antennas	$\theta_{mn,2}$	Azimuth of receiving antenna $RX_{m,2}$
I_{m_a}	Serial number of the activated antennas	k	Wave number
\mathbf{A}	Antenna selection matrix	λ	Wavelength
\mathbf{s}	Modulation symbol vector	\mathbb{G}	Symbol set of GSM
\mathbb{S}	Modulation symbol vector set	\mathbf{x}	Transmission vectors of GSM
q_{nn}	Distance between transmitting antenna TX_n and receiving antennas $RX_{n,1}$ and $RX_{n,2}$	\mathbf{w}	Circularly symmetric complex Gaussian noise vector
\mathbf{H}_1	Channel gain matrix from the transmitter to the first antenna in receiving antenna pairs	\mathbf{H}_2	Channel gain matrix from the transmitter to the second antenna in receiving antenna pairs
l_n	OAM state of an OAM wave emitted by the n^{th} transmitting antenna	ω_n	Optical waist radius of the OAM wave when the OAM state is l_n and $z=0$
$\mathbf{H}_{n,1}^{l_n}$	Channel gain between the first antenna in receiving antenna pairs and the n^{th} transmitting antenna	$\mathbf{H}_{n,2}^{l_n}$	Channel gain between the second antenna in receiving antenna pairs and the n^{th} transmitting antenna
$w_n(z)$	Radius where the amplitude of electromagnetic wave drops to $1/e$	σ	Angle between two receiving antennas in a pair of receiving antennas
$h_{mn,1}^{l_n}$	Channel gain between the first antenna in the m^{th} receiving antenna pair and the n^{th} transmitting antenna	$h_{mn,2}^{l_n}$	Channel gain between the second antenna in the m^{th} receiving antenna pair and the n^{th} transmitting antenna
\mathcal{N}	Number of activated antenna matrices	\mathcal{S}	Number of modulation symbol vectors
\mathcal{J}	Gain coefficient of the transmitting antenna	\mathcal{L}	Number of channel gain matrices
$q_{mn,1}$	Distance from receiving antenna $RX_{m,1}$ to transmitting antenna TX_n	$\phi_{m,1}$	Phase of the OAM beam detected by receiving antenna $RX_{m,1}$
$q_{mn,2}$	Distance from receiving antenna $RX_{m,2}$ to transmitting antenna TX_n	$\phi_{m,2}$	Phase of the OAM beam detected by receiving antenna $RX_{m,2}$

We ensure that $RX_{m,1}$, $RX_{m,2}$ antennas are in the circular area of the OAM beam transmitted by TX_n , so the relative position between receiving antenna pair $RX_{m,1}$, $RX_{m,2}$ and transmitting antenna TX_n satisfies $m=n$.

In the OAM-GSM system, multiple transmitting antennas are activated as activated antennas which transmit signals at each moment. Assuming that at a certain moment, M_a antennas are selected from the M transmitting antennas as activated antennas to transmit signals, then there are $\mathcal{N} = 2^{\lfloor \log_2(C_M^{M_a}) \rfloor}$ sets of transmitting antenna combinations for modulating information bits. The set consisting of matrices determined by the combinations of the activated antenna is represented as \mathbb{A} , which is called the antenna selection matrix set. The antenna selection matrix corresponding to the activated antenna selected at a certain moment is denoted as \mathbf{A} , and $\mathbf{A} \in \mathbb{C}^{M \times M_a}$, $\mathbf{A} \in \mathbb{A}$. The antenna selection matrix \mathbf{A} is selected from the antenna selection matrix set \mathbb{A} with a medium probability. In addition, \mathbf{A} is a sparse matrix, which contains only 0 or 1 element value. If $I_1, \dots, I_{M_a}, \dots, I_{M_a}$ represent the serial numbers of the activated antennas selected at a certain moment and I_{m_a} represents the antenna number of the m_a^{th} activated antenna, then values of element A_{ij} in row i and column j of matrix \mathbf{A} are

$$A_{ij} = \begin{cases} 1, & i = I_{m_a}, j = m_a, \\ 0, & \text{otherwise.} \end{cases} \quad (1)$$

The modulation symbol transmitted by each activated antenna adopts P -point constellation modulation, and the modulation symbol is selected from P constellation symbols with a medium probability. \mathbb{S} represents a set of all possible modulation symbol vectors transmitted by M_a activated antennas, and \mathbf{s} represents the modulation symbol vector transmitted by M_a activated antennas at a certain time, $\mathbf{s} \in \mathbb{C}^{M_a}$ and $\mathbf{s} \in \mathbb{S}$. The number of vectors contained in \mathbb{S} is $|\mathbb{S}| = P^{M_a}$ and \mathbf{s} is a modulation symbol vector selected from \mathbb{S} with a medium probability. In addition, if the OAM state of the OAM beam transmitted by the i^{th} transmitting antenna is l_i and the OAM state set is \mathcal{Q} which contains L OAM states, then l_i is selected

from L OAM states in \mathcal{Q} with a medium probability.

$\mathbf{H}_1 \in \mathbb{C}^{M \times M}$ is used to represent the channel gain matrix from the transmitter of the OAM-GSM system to the first antenna in all receiving antenna pairs, and $\mathbf{H}_2 \in \mathbb{C}^{M \times M}$ is used to represent the channel gain matrix from the transmitter of the OAM-GSM system to the second antenna in all receiving antenna pairs. For channel matrices $\mathbf{H}_1 = (\mathbf{H}_{1,1}^{l_1}, \mathbf{H}_{2,1}^{l_2}, \dots, \mathbf{H}_{M,1}^{l_M}) \in \mathbb{C}^{M \times M}$ and $\mathbf{H}_2 = (\mathbf{H}_{1,2}^{l_1}, \mathbf{H}_{2,2}^{l_2}, \dots, \mathbf{H}_{M,2}^{l_M}) \in \mathbb{C}^{M \times M}$ of the OAM-GSM system, the OAM wireless channel model proposed by Wang L et al. (2017) is used. $\mathbf{H}_{n,1}^{l_n} = [h_{n,1}^{l_n}, \dots, h_{mn,1}^{l_n}, \dots, h_{Mn,1}^{l_n}]^T \in \mathbb{C}^M$ is the n^{th} ($1 \leq n \leq M$) column vector in channel matrix \mathbf{H}_1 , representing the channel gain between the first antenna in all receiving antenna pairs and the n^{th} transmitting antenna TX_n . $h_{mn,1}^{l_n}$ represents the channel gain between the first antenna in the m^{th} receiving antenna pair and the n^{th} transmitting antenna. Similarly, $\mathbf{H}_{n,2}^{l_n} = [h_{n,2}^{l_n}, \dots, h_{mn,2}^{l_n}, \dots, h_{Mn,2}^{l_n}]^T \in \mathbb{C}^M$ is the n^{th} ($1 \leq n \leq M$) column vector in channel matrix \mathbf{H}_2 , representing the channel gain between the second antenna in all receiving antenna pairs and the n^{th} transmitting antenna TX_n . $h_{mn,2}^{l_n}$ represents the channel gain between the second antenna in the m^{th} receiving antenna pair and the n^{th} transmitting antenna. \mathcal{S} represents the gain coefficient of the transmitting antenna and is set as a constant.

Fig. 2 is the model diagram of OAM electromagnetic wave propagation in an OAM-GSM system. As shown in Fig. 2, $q_{mn,1}$ and $q_{mn,2}$ represent the distances from receiving antennas $RX_{m,1}$ and $RX_{m,2}$ to transmitting antenna TX_n , respectively. The distances between transmitting antenna TX_n and receiving antennas $RX_{n,1}$ and $RX_{n,2}$ are equal and are expressed by q_{nn} . $d_{mn,1}$ and $d_{mn,2}$ represent the radial distances from transmitting antenna TX_n to receiving antennas $RX_{m,1}$ and $RX_{m,2}$, respectively. The radial distances from transmitting antenna TX_n to receiving antennas $RX_{n,1}$ and $RX_{n,2}$ are equal, denoted by d_{nn} . ω_n represents the optical waist radius of the OAM electromagnetic

wave when the OAM state is l_n and $z=0$. $w_n(z)$ represents the radius where the amplitude of the electromagnetic wave drops to $1/e$. $\theta_{mn,1}$ and $\theta_{mn,2}$ represent the azimuth of receiving antenna pair $RX_{m,1}$ and $RX_{m,2}$, respectively. σ represents the angle between two receiving antennas in a pair of receiving antennas, l_n represents the OAM state of an OAM wave emitted by the n^{th} transmitting antenna, k represents the wave number, and λ represents the wavelength. According to the channel model of an OAM wireless communication system, the channel gain between the m^{th} receiving antenna pair $RX_{m,1}$, $RX_{m,2}$, and the n^{th} transmitting antenna TX_n is denoted as $h_{mn,1}^{l_n}$, $h_{mn,2}^{l_n}$, and expressed as Eq. (2). In an OAM-GSM system, the OAM states of OAM beams that can be emitted by transmitting antennas are selected from the OAM state set with a medium probability. In different time slots, the OAM states of OAM beams emitted by transmitting antennas may be different. Therefore, channel gain matrices \mathbf{H}_1 and \mathbf{H}_2 of the OAM-GSM system are related to the states of the OAM beams emitted by transmitting antennas. That is, at any moment, the OAM states of OAM beams selected by the transmitting antenna determine the channel matrix of the OAM-GSM system. Let \mathbb{H}_1 be the set of all possible \mathbf{H}_1 matrices and \mathbb{H}_2 the set of all possible \mathbf{H}_2 matrices. The channel gain matrix \mathbf{H}_1 of the OAM-GSM system is selected from channel gain matrix set \mathbb{H}_1 with a medium probability, and

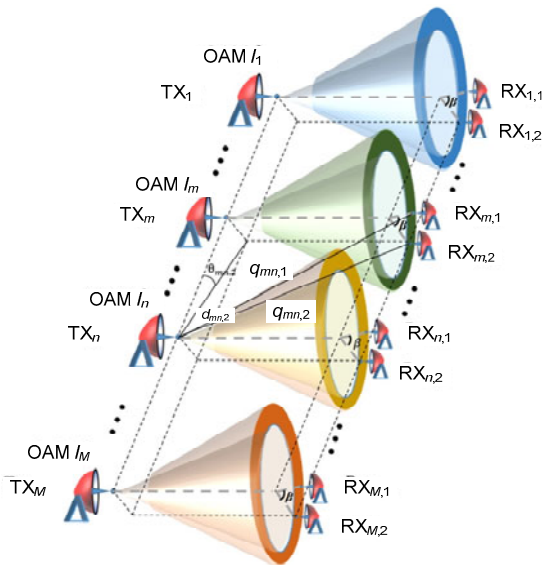


Fig. 2 Model diagram of OAM electromagnetic wave propagation in an OAM-GSM system

channel gain matrix \mathbf{H}_2 of the OAM-GSM system is selected from channel gain matrix set \mathbb{H}_2 with a medium probability, so $\mathbf{H}_1 \in \mathbb{H}_1$, $\mathbf{H}_2 \in \mathbb{H}_2$. Since the states of OAM beams emitted by transmitting antennas are selected from L OAM states with a medium probability, the number of channel gain matrices included in channel gain matrix sets \mathbb{H}_1 and \mathbb{H}_2 is $\mathcal{L} = L^M$.

$$h_{mn,1}^{l_n} = \begin{cases} \mathcal{J} \frac{\lambda}{4\pi q_{mn,1}} e^{-ikq_{mn,1}} e^{-il_n \pi/2}, & m = n, \\ \mathcal{J} \frac{\lambda}{4\pi q_{mn,1}} \left(\frac{d_{mn,1}}{d_{nn}} \right)^{|l_n|} \exp\left(-\frac{d_{mn,1}^2 - d_{nn}^2}{w_n^2(z)}\right) \\ \cdot \exp\left(-i \frac{\pi(d_{mn,1}^2 - d_{nn}^2)}{\lambda R_n(z)}\right) e^{-ikq_{nn}} e^{-il_n \theta_{mn,1}}, & m \neq n, \end{cases} \quad (2a)$$

$$R_n(z) = z \left[1 + \left(\frac{\pi \omega_n^2}{\lambda z} \right)^2 \right], \quad (2b)$$

$$h_{mn,2}^{l_n} = \begin{cases} \mathcal{J} \frac{\lambda}{4\pi q_{mn,2}} e^{-ikq_{mn,2}} \exp\left(-il_n \left(\frac{\pi}{2} + \sigma \right)\right), & m = n, \\ \mathcal{J} \frac{\lambda}{4\pi q_{mn,2}} \left(\frac{d_{mn,2}}{d_{nn}} \right)^{|l_n|} \exp\left(-\frac{d_{mn,2}^2 - d_{nn}^2}{w_n^2(z)}\right) \\ \cdot \exp\left(-i \frac{\pi(d_{mn,2}^2 - d_{nn}^2)}{\lambda R_n(z)}\right) e^{-ikq_{nn}} e^{-il_n \theta_{mn,2}}, & m \neq n. \end{cases} \quad (2c)$$

Let \mathbb{G} be the symbol set of GSM. This represents the set of all possible transmission vectors and $\mathbf{x} \in \mathbb{C}^M$ represents the signal vectors emitted by the transmitting antennas, $\mathbf{x} \in \mathbb{G}$. Any \mathbf{x} can be expressed as the product of antenna selection matrix \mathbf{A} and modulation symbol vector $\mathbf{s} = [s_1, s_2, \dots, s_{M_a}]^T \in \mathbb{C}^{M_a}$, that is, $\mathbf{x} = \mathbf{A}\mathbf{s}$. Then for the GSM symbol set, $\mathbb{G} = \{\mathbf{x} : \mathbf{x} = \mathbf{A}\mathbf{s}, \mathbf{A} \in \mathbb{A}, \mathbf{s} \in \mathbb{S}\}$.

Therefore, the input and output equations of the OAM-GSM system can be expressed as

$$\mathbf{Y}_1 = \mathbf{H}_1 \mathbf{x} + \mathbf{W} = \mathbf{H}_1 \mathbf{A} \mathbf{s} + \mathbf{W}, \quad (3)$$

$$\mathbf{Y}_2 = \mathbf{H}_2 \mathbf{x} + \mathbf{W} = \mathbf{H}_2 \mathbf{A} \mathbf{s} + \mathbf{W}. \quad (4)$$

In Eqs. (3) and (4), Y_1 represents the signals received by the first antenna in all receiving antenna pairs and Y_2 represents the signals received by the second antenna in all receiving antenna pairs. The channel gain matrices H_1 and H_2 remain unchanged in a time slot. $w = [w_1, w_2, \dots, w_M]^T \in \mathbb{C}^M$ represents a circularly symmetric complex Gaussian noise vector. Each element in w has a mean of 0 and a variance of σ_w^2 . In Eqs. (3) and (4), the signal vector x emitted by a transmitter is independent of channel matrices $H_1 \in \mathbb{C}^{M \times M}$ and $H_2 \in \mathbb{C}^{M \times M}$. At any moment, antenna selection matrix A is selected with a medium probability from antenna selection matrix set \mathbb{A} , and a modulation symbol vector s is selected with a medium probability from modulation symbol vector set \mathbb{S} . Therefore, A and s are also independent of each other.

2.2 OAM-GSM system transmission mechanism

For a traditional GSM system, assuming that the number of transmitting antennas is M and the number of activated antennas is M_a , the modulation symbols transmitted by each activated antenna are modulated with P -point constellation modulation. Then a binary bit stream of the system will be divided into two parts for transmission. $B_1^{\text{GSM}} = \lfloor \log_2 (C_M^{M_a}) \rfloor$ bits are used to select an activated antenna combination and $B_2^{\text{GSM}} = M_a \lfloor \log_2 P \rfloor$ bits are used to select modulation symbols. Therefore, the transmission rate of the OAM-GSM system is

$$R_{\text{GSM}} = \lfloor \log_2 (C_M^{M_a}) \rfloor + M_a \lfloor \log_2 P \rfloor. \quad (5)$$

In an OAM-GSM system, we introduce OAM states, using different OAM states for encoding and modulation. Some bits in a binary bit stream can be mapped to different OAM states, so that information transmission can be achieved by selecting different OAM states. The OAM state of the OAM beam transmitted by each antenna is selected from L OAM states in OAM state set \mathcal{Q} with a medium probability, so each transmitting antenna can transmit $\lfloor \log_2 L \rfloor$ bits of information by selecting OAM states. In addition, in the OAM-GSM system, part of bits in the binary bit stream are used to select antennas and part of bits are

used to select constellation symbols.

In general, at a certain moment in an OAM-GSM system, M_a activated antennas are selected from M transmitting antennas for data transmission, and there are a total of $C_M^{M_a}$ activated antenna combinations. To modulate information, a total of $\mathcal{N} = 2^{\lfloor \log_2 (C_M^{M_a}) \rfloor}$ sets of transmitting antenna combinations are selected as activated antenna combinations to transmit information. Therefore, as shown in Fig. 3, in an OAM-GSM system, the total information bits at each moment are divided into three parts for transmission.

$B_1 = \lfloor \log_2 (C_M^{M_a}) \rfloor$ bits are used to select a group of activated antennas, $B_2 = M_a \lfloor \log_2 P \rfloor$ bits are used to transmit M_a constellation symbols with P -point constellation modulation, and $B_3 = M_a \lfloor \log_2 L \rfloor$ bits are used to select M_a OAM states.

Thus, the transmission rate of an OAM-GSM system is

$$R_{\text{OAM-GSM}} = \lfloor \log_2 (C_M^{M_a}) \rfloor + M_a \lfloor \log_2 P \rfloor + M_a \lfloor \log_2 L \rfloor, \quad (6)$$

where $\lfloor \cdot \rfloor$ means round down.

In Fig. 3, the number of transmitting antennas contained in the uniform linear array at the transmitter is $M=4$, the number of antennas activated at a certain moment is $M_a=2$, and the OAM state set \mathcal{Q} contains two OAM states, 1 and -1 . The modulation symbol transmitted by each activated antenna is modulated by 4PSK technology. From the above description, this system can transmit $\lfloor \log_2 C_4^2 \rfloor + 2 \lfloor \log_2 4 \rfloor + 2 \lfloor \log_2 2 \rfloor = 8$ bits.

2.3 OAM-GSM system reception mechanism

Compared with a traditional GSM system, the OAM-GSM system not only loads information on the activated antenna combination and constellation symbols, but also loads part of the information on the OAM states of the transmitted OAM beams. Therefore, the receiver of the OAM-GSM system needs to detect all information sent by the transmitter, including information of the activated antenna combination, modulation symbols, and OAM states.

In the OAM-GSM system model, OAM states and the channel matrix of the OAM-GSM system are

inseparable. We assume that the channel gain matrix set \mathbb{H} , activated antenna matrix set \mathbb{A} , and modulation symbol vector signal set \mathbb{S} of the OAM-GSM system are known at the receiver. The maximum likelihood method can be used to detect the information sent by the transmitter. By exhaustively searching \mathbb{H} , \mathbb{A} , and \mathbb{S} , the estimated values of channel gain matrix \mathbf{H}_1 , antenna selection matrix \mathbf{A} , and modulation symbol vector \mathbf{s} can be calculated:

$$\left[\hat{\mathbf{H}}_1, \hat{\mathbf{A}}, \hat{\mathbf{s}} \right] = \arg \min_{\substack{1 \leq k \leq \mathcal{L}, 1 \leq i \leq \mathcal{N}, 1 \leq j \leq \mathcal{S}}} \|\mathbf{y} - \mathbf{H}_k \mathbf{A}_i \mathbf{s}_j\|^2, \quad (7)$$

where \mathbf{y} is the signal detected by the receiver, $\hat{\mathbf{H}}_1$, $\hat{\mathbf{A}}$, and $\hat{\mathbf{s}}$ are the demodulated channel gain matrix, antenna selection matrix, and symbol vector, respectively. Through $\hat{\mathbf{H}}_1$, $\hat{\mathbf{A}}$, and $\hat{\mathbf{s}}$, transmitting antenna indices, OAM states, and the signal transmitted using traditional modulation methods can be obtained. However, because of the use of exhaustive search, the complexity of the maximum likelihood detection method is very high and each detection requires $\mathcal{S}\mathcal{L}\mathcal{N}$ times of complex multiplication. \mathcal{N} , \mathcal{S} , and \mathcal{L} represent the number of activated antenna matrices in \mathbb{A} , number of modulation symbol vectors in \mathbb{S} , and

number of channel gain matrices in \mathbb{H} , respectively. This approach is difficult to implement when the number of transmitting antennas, OAM states, or modulation symbols is large.

For the OAM-GSM system model designed in this study, we propose a separate detection method to detect traditional modulation symbols, the activated antenna matrix, and OAM states (Cover and Thomas, 2006). Both antennas in a receiving antenna pair are placed in the ring area of the OAM beam transmitted by a corresponding transmitting antenna, so the signal strengths received by two antennas in the same receiving antenna pair are equal. Therefore, when detecting the active mode and traditional modulation symbols, only the signal received by one of the antennas in a receiving antenna pair is required to participate in the calculation. This paper uses signals received by the first antenna in receiving antenna pairs to participate in the calculation. From the phases of the OAM beam detected by two receiving antennas in a receiving antenna pair, the OAM state of the OAM electromagnetic wave can be judged by the phase gradient method (Edfors and Johansson, 2012):

$$\hat{k} = \arg \max_{1 \leq k \leq \mathcal{N}} \left(\sum_{i=1}^{M_A} |y_{C(k,i),1}|^2 \right). \quad (8)$$

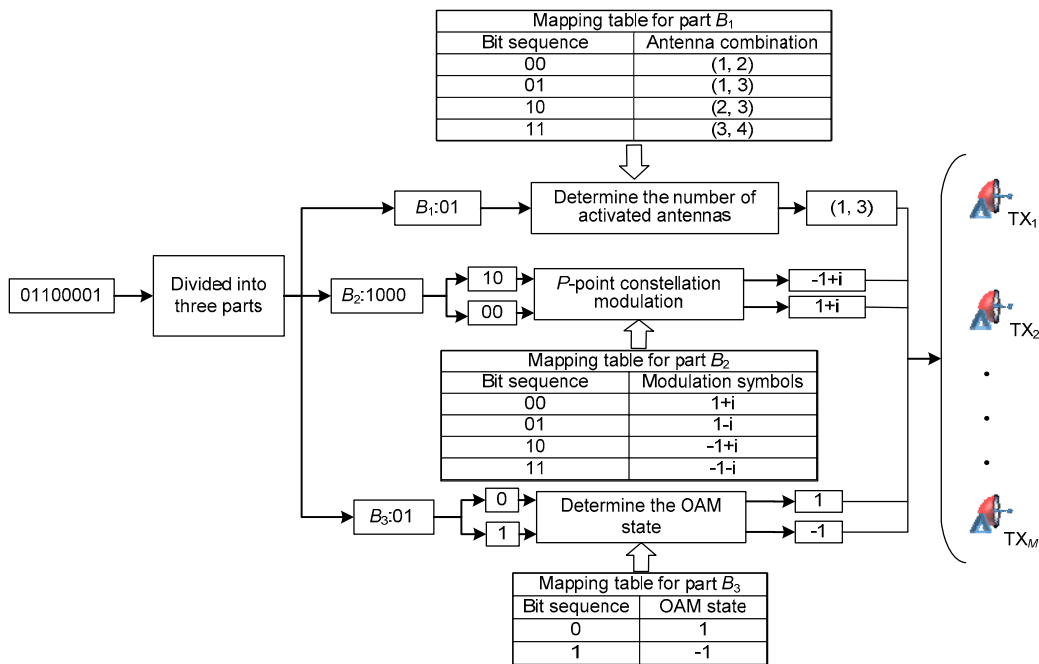


Fig. 3 Schematic of bit mapping at the transmitter of the OAM-GSM system

First, the activation mode adopted by the transmitter can be determined according to the received signal strength, as shown in Eq. (8). $C(k, i)$ represents the sequence number of the i^{th} activated antenna in the activated antenna combination represented by the k^{th} activated antenna matrix in set \mathbb{A} . $y_{C(k,i),1}$ is the signal received by the first antenna in the receiving antenna pair corresponding to the i^{th} activated antenna in the activated antenna combination represented by the k^{th} activated antenna matrix in set \mathbb{A} . \hat{k} represents that the demodulated antenna selection matrix is the \hat{k}^{th} one in set \mathbb{A} .

After determining the antenna selection matrix, the gradient phase method can be used to demodulate the OAM state according to the phase of the OAM beam detected by the receiving antenna corresponding to the activated antenna, as shown in Eq. (9):

$$\hat{l}_m = \frac{\phi_{m,1} - \phi_{m,2}}{\sigma}, \quad (9)$$

where $\phi_{m,1}$ and $\phi_{m,2}$ are the phases of the OAM beam detected by receiving antennas $RX_{m,1}$ and $RX_{m,2}$, respectively. \hat{l}_m represents the demodulated state of

the OAM beam emitted by the m^{th} transmitting antenna.

According to the antenna selection matrix and OAM state demodulated in the previous two steps, combined with the channel gain calculation method given by Eq. (2), the channel gain matrix can be calculated. Then, the maximum likelihood method is used to demodulate the modulation symbol vector, as shown in Eq. (10):

$$\hat{s} = \min_{1 \leq j \leq S} \| \mathbf{y} - \mathbf{H}_1 \mathbf{A} \mathbf{s}_j \|^2, \quad (10)$$

where \mathbf{H}_1 and \mathbf{A} are the channel gain matrix and antenna selection matrix demodulated according to the first two steps respectively, \hat{s} is the symbol vector demodulated, and the transmission symbol transmitted by the traditional modulation method can be obtained through \hat{s} .

In Fig. 4, the number of receiving antenna pairs at the receiver is $M=4$ and the number of antennas activated at a certain time is $M_a=2$. The OAM state set Q includes two OAM states, which are 1 and -1 . The modulation symbol transmitted by each activated antenna is modulated by 4PSK technology.

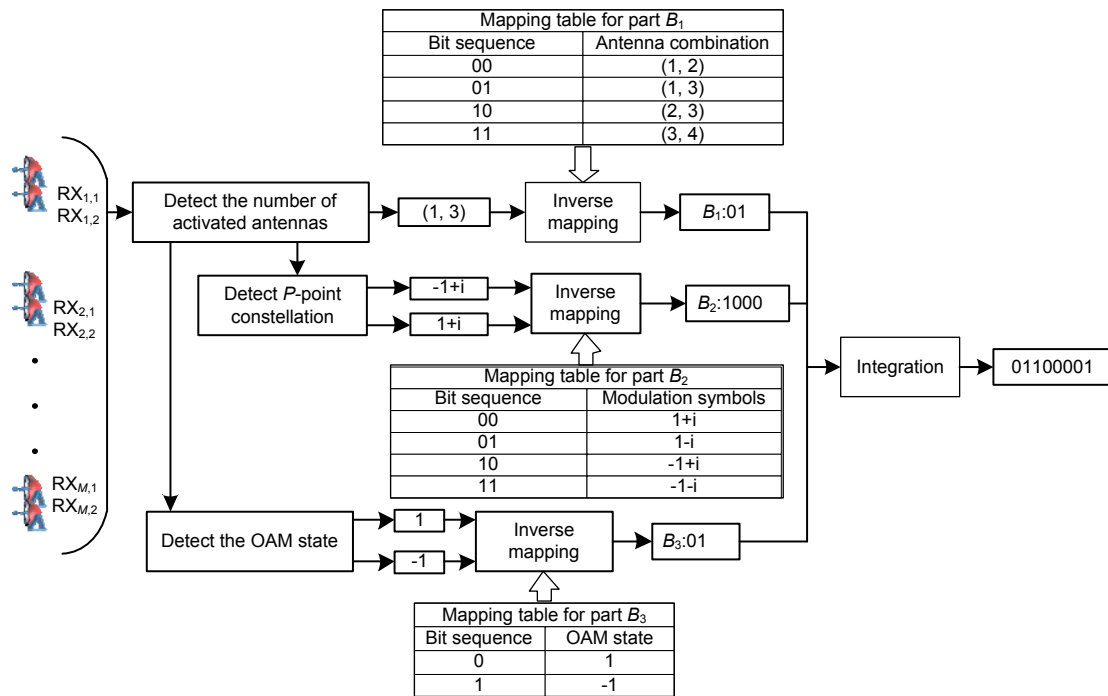


Fig. 4 Structure diagram of the receiver of the OAM-GSM system

3 Capacity, energy efficiency, and BER analysis of the OAM-GSM system

3.1 Channel capacity analysis of the OAM-GSM system

It is assumed that the signal vector \mathbf{x} emitted by the transmitter is formed by the product of the i^{th} matrix \mathbf{A}_i in the activated antenna matrix set \mathbb{A} and the j^{th} vector \mathbf{s}_j in the modulation symbol vector signal set \mathbb{S} . Meanwhile, it is assumed that the channel matrix formed by the OAM state of the OAM beam selected by the activated antenna is \mathbf{H}_k , the k^{th} matrix in the set of channel gain matrix \mathbb{H}_1 . The signal vector \mathbf{y} received by the first antenna in a receiving antenna pair can be expressed as follows:

$$\mathbf{y} = \mathbf{H}_k \mathbf{A}_i \mathbf{s}_j + \mathbf{W}. \quad (11)$$

Regardless of the classical Shannon channel capacity or the channel capacity of a traditional MIMO system, when input symbols obey a Gaussian distribution, the channel capacity reaches its maximum value (Cover and Thomas, 2006). The OAM-GSM system proposed in this study is different from traditional MIMO systems. The special feature is that spatial symbols, modulation symbols, and OAM state values transmitted through antennas are all integers. That is, the antenna serial number, modulation symbol vector, and OAM state value are not subject to a Gaussian distribution. This means that for the channel capacity of the OAM-GSM system, its value depends on a mixture of discrete and continuous input. For simplicity, the OAM-GSM system channel can be regarded as a discrete input continuous output memoryless channel, so the channel capacity of the OAM-GSM system can be derived as (Gallager et al., 1968)

$$C = \max_{p(\mathbf{s}_j), p(\mathbf{A}_i), p(\mathbf{H}_k)} \sum_{k=1}^{\mathcal{L}} \sum_{j=1}^{\mathcal{S}} \sum_{i=1}^{\mathcal{N}} \int_{-\infty}^{\infty} p(\mathbf{y}, \mathbf{H}_k, \mathbf{A}_i, \mathbf{s}_j) \delta \mathbf{y}, \quad (12a)$$

$$\delta = \log_2 \frac{p(\mathbf{y} | \mathbf{H}_k, \mathbf{A}_i, \mathbf{s}_j)}{\sum_{k_1=1}^{\mathcal{L}} \sum_{j_1=1}^{\mathcal{S}} \sum_{i_1=1}^{\mathcal{N}} p(\mathbf{y}, \mathbf{H}_{k_1}, \mathbf{A}_{i_1}, \mathbf{s}_{j_1})}. \quad (12b)$$

Theorem 1 Assume that all elements in \mathbf{W} in the input and output equations of the system are additive white Gaussian noise with a mean of 0 and variance of σ_w^2 . If the symbol vector \mathbf{s}_i , antenna selection matrix \mathbf{A}_i , and channel matrix \mathbf{H}_k are known, then the channel capacity formula can be derived as

$$C = \log_2 \mathcal{L} \mathcal{S} \mathcal{N} - \sum_{k=1}^{\mathcal{L}} \sum_{j=1}^{\mathcal{S}} \sum_{i=1}^{\mathcal{N}} \mathbb{E}(\mathbf{W}) \log_2 \sum_{k_1=1}^{\mathcal{L}} \sum_{j_1=1}^{\mathcal{S}} \sum_{i_1=1}^{\mathcal{N}} e^{\psi}, \quad (13a)$$

$$\psi = \frac{\|\mathbf{W}\|^2 - \|\mathbf{H}_k \mathbf{A}_i \mathbf{s}_j - \mathbf{H}_{k_1} \mathbf{A}_{i_1} \mathbf{s}_{j_1} + \mathbf{W}\|^2}{\sigma_w^2}. \quad (13b)$$

The proof of Theorem 1 is given in Appendix A.

3.2 Energy efficiency analysis of the OAM-GSM system

The energy efficiency of the proposed OAM-GSM mmWave communication system is analyzed below and compared with that of traditional GSM communication systems. Assuming that all transmitting antennas distribute transmission power equally, then the power consumed by a multi-antenna transmitter is (Simon and Alouini, 2005)

$$p^{\text{total}} = M_a p_a + \tau M_a p, \quad (14)$$

where p_a is the power consumed by a circuit related to an activated antenna, p the transmit power of an activated antenna, a the number of activated antennas, and τ the slope of the load-dependent power consumption. Compared with transmitting antennas, the power consumed by receiving antennas is very small and can be ignored (Simon and Alouini, 2005; Stavridis et al., 2012). The energy efficiency of a communication system can be expressed as

$$\eta = B \cdot C(M_a p) / p^{\text{total}}, \quad (15)$$

where $M_a p$ represents the total transmit power, B represents the bandwidth, and $C(M_a p)$ is the capacity in terms of the total transmit power. Therefore, the energy efficiency of the OAM-GSM mmWave communication system can be expressed as

$$\eta_{\text{OAM-GSM}} = \frac{B \cdot C_{\text{OAM-GSM}}(M_a p)}{M_a p a + \tau M_a p}, \quad (16)$$

where $C_{\text{OAM-GSM}}(M_a p)$ can be derived from the analysis of the channel capacity of the OAM-GSM system in Appendix A.

For a traditional GSM system with the same number of activated antennas as in the OAM-GSM mmWave wireless communication system, its energy efficiency can be expressed as

$$\eta_{\text{GSM}} = \frac{B \cdot C_{\text{GSM}}(M_a p)}{M_a p a + \tau M_a p}. \quad (17)$$

$C_{\text{GSM}}(M_a p)$ can be obtained from the analysis of the channel capacity of a traditional GSM system (Xiao et al., 2014).

3.3 BER analysis of the OAM-GSM system

For the proposed OAM-GSM mmWave communication system, the receiver extracts the transmitted symbols from the received signal and demodulates according to the activated antenna combination, OAM states, and constellation symbols. In the proposed OAM-GSM system, determination of the transmitting antenna index depends on the power strength of receiving antenna pairs. Based on the OAM-GSM system, the receiving antenna corresponding to the transmitting antenna is arranged in the intensity focusing circular area where the OAM beam intensity is the largest. It is assumed that the channel gain matrix, activated antenna matrix, and modulation symbol vector signal sets of the OAM-GSM system are known at the receiver. Separate detection can be used to handle the detection of the traditional modulation symbol, activated antenna matrix, and OAM state separately (Zhang R et al., 2015).

For future calculations, e_{ant}^s is defined to represent the symbol error rate (SER) of the space signal part. \tilde{e}_{mod}^s is defined to represent the SER of the modulation symbol when considering whether the activated antenna is detected correctly. \tilde{e}_{OAM}^s is defined to represent the SER of the OAM state symbol when considering whether the activated antennas are detected correctly. $k_{\text{ant}} = \left\lfloor \log_2 C_{M_a}^{M_a} \right\rfloor$ is defined to

represent the number of bits used to select the activated antenna combination, $k_{\text{mod}} = \log_2 P$ the number of bits used to select P -point constellation modulation symbols, and $k_{\text{OAM}} = \log_2 L$ the number of bits used to select OAM states.

Theorem 2 If separate detection is used to handle the detection of the traditional modulation symbol, activated antenna matrix, and OAM state, then the BER of the OAM-GSM system can be expressed as

$$e^b = \frac{\delta_{k_{\text{ant}}} e_{\text{ant}}^s + M_a \tilde{e}_{\text{mod}}^s + M_a \tilde{e}_{\text{OAM}}^s}{k_{\text{ant}} + M_a k_{\text{mod}} + M_a k_{\text{OAM}}}, \quad (18)$$

where $\delta_{k_{\text{ant}}} = \delta_{k_{\text{ant}}-1} + (2^{\delta_{k_{\text{ant}}-1}} - \delta_{k_{\text{ant}}-1}) / (2^{\delta_{k_{\text{ant}}}} - 1)$, $\delta_0 = 0$.

The proof of Theorem 2 is given in Appendix B.

We simulate the BER of the OAM-GSM system and compare it with that of a traditional GSM system. In the simulation, both the transmitter and receiver of the traditional GSM system use uniform linear antenna arrays, and the number of antennas at the transmitter is the same as that at the transmitter in the OAM-GSM system. The difference between the traditional GSM and OAM-GSM systems is that OAM antennas are configured in the transmitter and receiver in an OAM-GSM system to realize transmission and reception of OAM beams, while the transmitter and receiver in a GSM system use the antennas usually used. In the simulation, the number of activated antennas at a certain moment in a traditional GSM system is the same as that of activated antennas in the OAM-GSM system. The traditional GSM system and the OAM-GSM system use the same signal modulation strategy of the same order. Default parameter settings in the simulation are shown in Table 2 (Liu et al., 2016).

Fig. 5 shows how the BER of the OAM-GSM and traditional GSM systems varies with the signal-to-noise ratio (SNR). The simulation results show that the BER of the OAM-GSM and traditional GSM systems decreases with the increase of SNR. When SNR is smaller than or equal to 6 dB, the BER of the OAM-GSM system is larger than that of a traditional GSM system. When SNR is greater than 6 dB, the BER of the OAM-GSM system is smaller than that of a traditional GSM system. When SNR is 15 dB, compared with the traditional GSM system, the BER of the OAM-GSM system drops by 91.5%.

Table 2 Simulation parameters

Parameter	Value
Carrier frequency (GHz)	70
Bandwidth (GHz)	1
Transmission distance (m)	50
Number of optional OAM states	2
Set of OAM states	(10, 30)
Noise power spectral density (dBm/Hz)	-174
Distance between transmitting antennas	20λ
Number of transmitting antennas	4
Number of receiving antenna pairs	4
Number of antennas activated	2
Modulation type	4PSK
Power consumed by a circuit related to an activated antenna (W)	6.8
Slope of the load-dependent power consumption	4.0

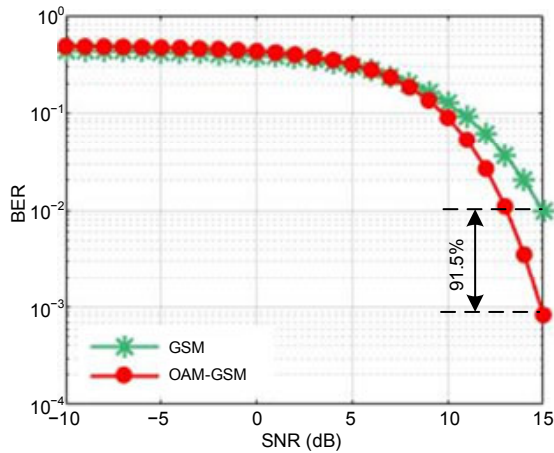


Fig. 5 BER vs. SNR in the OAM-GSM system and traditional GSM system

Fig. 6a shows how the BER of an OAM-GSM system changes with SNR when the number of optional OAM states is different. Simulation results show that when SNR is smaller than or equal to 9 dB and is fixed, the BER of the OAM-GSM system decreases with the increase of the number of optional OAM states. When SNR is greater than or equal to 14 dB and is fixed, the BER of the OAM-GSM system increases with the increase of the number of optional OAM states.

Fig. 6b shows the situation where the BER of the OAM-GSM system changes with SNR under different modulation modes of P -point constellation modulation. The simulation results show that under the same SNR, the BER of the OAM-GSM system decreases with the increase of the point number in the P -point constellation modulation method.

In the actual process, we can increase the number of transmitting antennas and the number of activated antennas to achieve a larger channel capacity. Considering the case of using a different number of transmitting antennas, the simulation results are shown in Fig. 6c.

Fig. 6c shows how the BER of the OAM-GSM system varies with SNR when the number of transmitting antennas is different. Simulation results show that the BER of the OAM-GSM system increases with the increase of the number of transmitting antennas when SNR is unchanged.

3.4 OAM-GSM system based on channel flip precoding

Through the simulation analysis of the BER performance of an OAM-GSM system, it can be

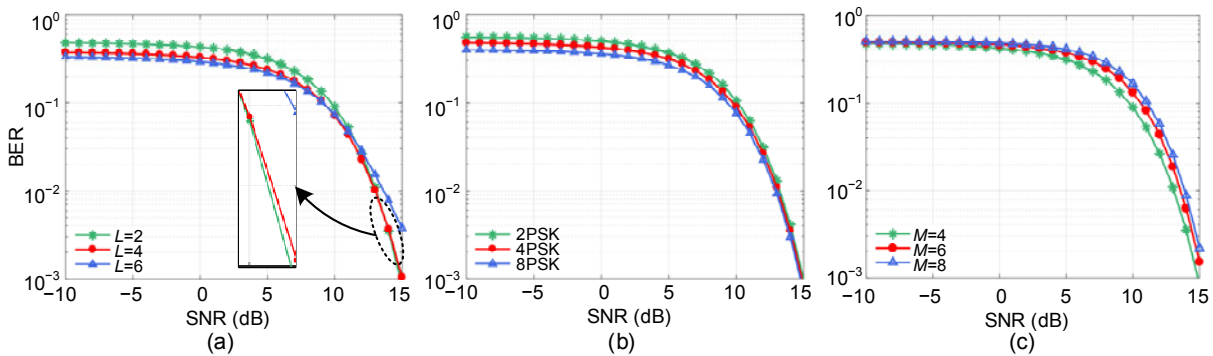


Fig. 6 BER of the OAM-GSM system changing with SNR considering different numbers of optional OAM states (a), different modulation modes of P -point constellation modulation (b), and different numbers of transmitting antennas (c)

known that the BER of the system increases with the increase of the number of transmitting antennas with other conditions unchanged. With the increase of bandwidth, the interference in the channel will increase, and the BER performance of the system will become worse. To reduce the BER when there is a large number of transmitting antennas, we propose a precoding solution for the OAM-GSM system.

After adding a transmitter precoder, e_{ant}^s is defined to represent the SER of the spatial signal part of the system. \tilde{e}_{mod}^s is defined to represent the SER of the modulation symbol when considering whether the activated antennas are detected correctly. \tilde{e}_{OAM}^s is defined to represent the SER of the OAM state symbol when considering whether the activated antennas are detected correctly.

The precoding matrix is (An et al., 2017)

$$P = H_1^H (H_1 H_1^H)^{-1}. \quad (19)$$

The signal received by the receiver can be expressed as

$$y_1 = H_1 P A s + W. \quad (20)$$

Substituting Eq. (19) into Eq. (20) gives

$$y_1 = A s + W. \quad (21)$$

Theorem 3 If we add a channel flip precoding module to the OAM-GSM system, then the BER of

the system can be expressed as

$$\dot{e}^b = \frac{\delta_{k_{\text{ant}}} \tilde{e}_{\text{ant}}^s + M_a \tilde{e}_{\text{mod}}^s + M_a \tilde{e}_{\text{OAM}}^s}{k_{\text{ant}} + M_a k_{\text{mod}} + M_a k_{\text{OAM}}}, \quad (22)$$

where $\delta_{k_{\text{ant}}} = \delta_{k_{\text{ant}-1}} + (2^{\delta_{k_{\text{ant}-1}}} - \delta_{k_{\text{ant}-1}}) / (2^{\delta_{k_{\text{ant}}}} - 1)$, $\delta_0 = 0$.

The proof of Theorem 3 is given in Appendix C.

The BER performance of the OAM-GSM system based on channel flip precoding is simulated and compared with that of the OAM-GSM system without precoding. In the simulation, default parameters are the same as those in the BER performance simulation (Table 2).

Fig. 7a shows the curves of the BER of the OAM-GSM system with or without precoding changing with the SNR when the number of transmitting antennas is different. Fig. 7b shows the curve of the BER of the OAM-GSM system with or without precoding changing with the SNR when the number of optional OAM states is 6. Fig. 7c shows the curve of the BER of the OAM-GSM system with or without precoding changing with the SNR when the constellation modulation method used is 4PSK.

The simulation results show that under the same SNR condition, the BER of the OAM-GSM system with precoding is smaller than that of the OAM-GSM system without precoding. When the SNR is 15 dB, compared with the OAM-GSM system without precoding, the BER of the OAM-GSM system with precoding is reduced by 99.9%.

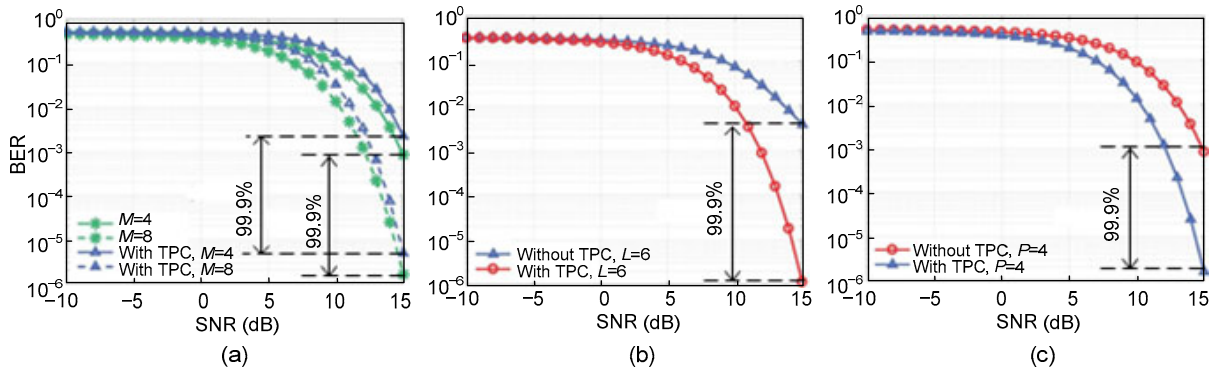


Fig. 7 BER of the OAM-GSM system with or without precoding changing with SNR considering different numbers of transmitting antennas (a), different numbers of optional OAM states (b), and different modulation modes of P -point constellation modulation (c) (TPC: transmitter precoder)

4 Performance simulation and analysis of the OAM-GSM system

In this section we simulate the channel capacity and energy efficiency of the system based on the OAM-GSM system and compare them with the channel capacity and energy efficiency of a traditional GSM system. Default parameters are the same as in the BER performance simulation (Table 2).

Fig. 8 shows how the channel capacity of the OAM-GSM communication system varies with the transmission SNR when different P -point constellation modulation methods are used. Simulation results show that the channel capacity of the OAM-GSM system gradually increases with the increase of the SNR when the selected constellation modulation method remains unchanged. When the SNR is greater than or equal to 8 dB, the BER of the OAM-GSM system increases with the increase of the point number in the P -point constellation modulation method.

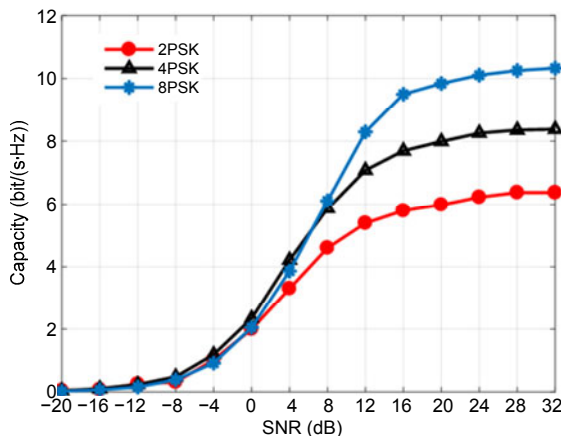


Fig. 8 Capacity of the OAM-GSM system with respect to the transmission SNR considering the P -point constellation modulation method

Fig. 9 shows how the channel capacity of the OAM-GSM system changes with the transmission distance when the number of transmitting antennas in the uniform linear array at the transmitter is different. Simulation results show that when the number of transmitting antennas is fixed, the channel capacity of the OAM-GSM system increases first and then decreases with the increase of the transmission distance. When the transmission distance is fixed, the channel capacity of the OAM-GSM system increases with the increase of the number of transmitting antennas.

Fig. 10 shows how the channel capacity of the OAM-GSM, OAM-SM, and traditional GSM systems varies with the SNR. Simulation results show that the channel capacity of the three systems gradually increases with the increase of SNR. For the OAM-GSM system, the channel capacity increases with the increase in the number of optional OAM states and is always greater than those of the OAM-SM system and the traditional GSM system. When SNR is 32 dB, compared with the traditional GSM system, the channel capacity of the OAM-GSM system with an optional OAM state number of 2 is increased by 42%, and the channel capacity of the OAM-GSM system with an optional OAM state number of 4 is increased by 80%. Compared with the SM system, the channel capacity of the OAM-GSM system with an optional OAM state number of 4 is increased by 177%.

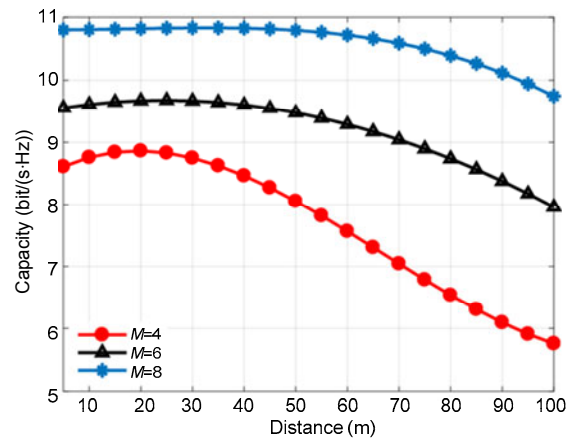


Fig. 9 Capacity of the OAM-GSM system with respect to the transmission distance considering different numbers of transmitting antennas

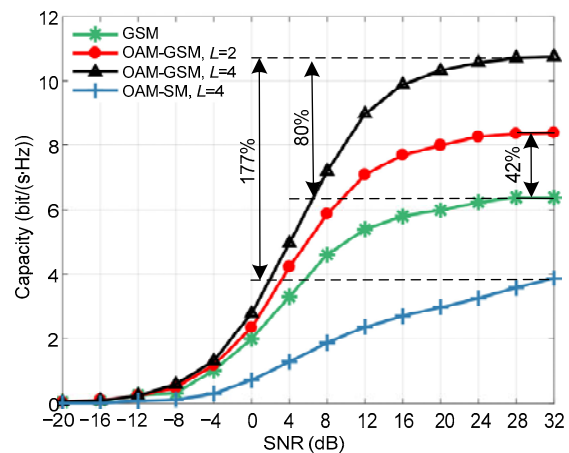


Fig. 10 Capacity of the OAM-GSM system, OAM-SM system, and traditional GSM system with respect to the transmission SNR

Fig. 11 shows how the channel capacity of the OAM-GSM, OAM-SM, and traditional GSM systems varies with the transmission distance. Simulation results show that the channel capacity of the OAM-GSM and traditional GSM systems increases first and then decreases with the increase of transmission distance. The channel capacity of the OAM-SM system decreases with the increase of the transmission distance. When the transmission distance is fixed, the channel capacity of the OAM-GSM system is always higher than those of the OAM-SM and GSM systems. When the transmission distance reaches 90 m, compared with the traditional GSM system, the channel capacity of the OAM-GSM system with an optional OAM state number of 2 is increased by 47%, and the channel capacity of the OAM-GSM system with an optional OAM state number of 4 is increased by 69%. Compared with the OAM-SM system, the channel capacity of the OAM-GSM system with an optional OAM state number of 4 is increased by 183%.

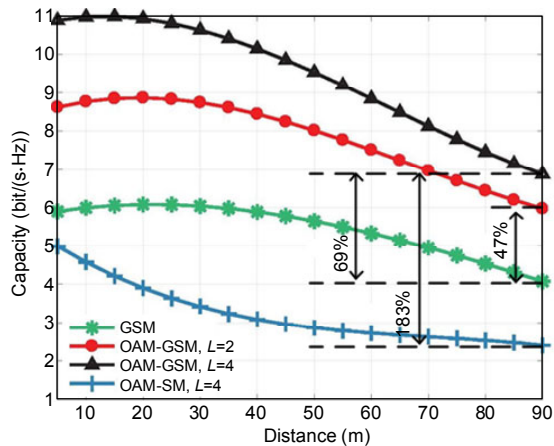


Fig. 11 Capacity of the OAM-GSM system, OAM-SM system, and traditional GSM system with respect to the transmission distance

Fig. 12 shows how the energy efficiency of the OAM-GSM, OAM-SM, and traditional GSM systems varies with SNR. Simulation results show that the energy efficiency of the OAM-GSM, OAM-SM, and traditional GSM systems increases first and then decreases with the increase of the transmission SNR, and there is a maximum energy efficiency. Compared with the traditional GSM system, the maximum energy efficiency of the OAM-GSM system with an optional OAM state number of 2 is increased by 31%,

and the maximum energy efficiency of the OAM-GSM system with an optional OAM state number of 4 is increased by 54%. Compared with the OAM-SM system, the maximum energy efficiency of the OAM-GSM system with an optional OAM state number of 4 is increased by 113%.

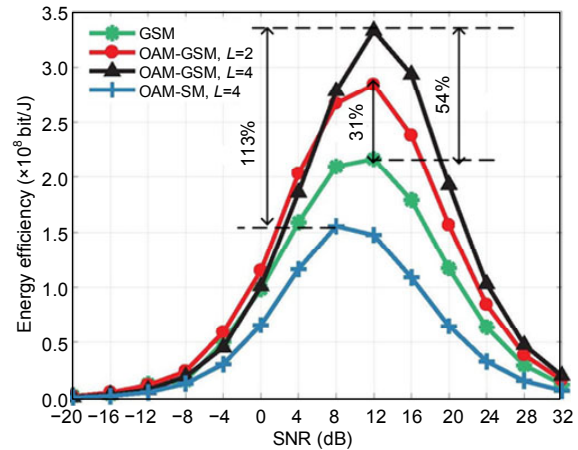


Fig. 12 Energy efficiency of the OAM-GSM system, OAM-SM system, and traditional GSM system with respect to the transmission SNR

5 Conclusions

In this paper, inspired by the idea of using OAM states to encode and decode signals, an OAM-GSM mmWave wireless communication system is designed. The channel capacity, energy efficiency, and BER performance of the proposed OAM-GSM mmWave wireless communication system are derived and simulated. The BER model of an OAM-GSM system based on channel flip precoding is established. Compared with traditional GSM systems, the OAM-GSM mmWave wireless communication system offers a significant performance improvement. Numerical results show that compared with the traditional GSM communication system, the OAM-GSM system has more complex transmission and reception mechanisms, but the channel capacity and maximum energy efficiency are increased by 80% and 54%, respectively, and the BER drops by 91.5%. A channel precoding algorithm can significantly reduce the BER of the OAM-GSM system. The OAM-GSM mmWave wireless communication system designed in this study can be used as a candidate solution for future

mobile networks. In the realization of the OAM-GSM mmWave wireless communication system, how to achieve perfect alignment of the transmitting antenna array and receiving antenna array is a challenge that requires further research.

Contributors

Qi ZHANG and Xusheng XIONG designed the research and processed the data. Qi ZHANG drafted the manuscript. Qiang LI and Xusheng XIONG helped organize the manuscript. Qiang LI, Tao HAN, and Yi ZHONG revised and finalized the paper.

Compliance with ethics guidelines

Qi ZHANG, Xusheng XIONG, Qiang LI, Tao HAN, and Yi ZHONG declare that they have no conflict of interest.

References

- Allen B, Tennant A, Bai Q, et al., 2014. Wireless data encoding and decoding using OAM modes. *Electron Lett*, 50(3):232-233. <https://doi.org/10.1049/el.2013.3906>
- Allen L, Beijersbergen MW, Spreeuw RJC, et al., 1992. Orbital angular momentum of light and the transformation of Laguerre-Gaussian laser modes. *Phys Rev A*, 45(11): 8185-8189. <https://doi.org/10.1103/PhysRevA.45.8185>
- An ZC, Wang J, Wang JT, et al., 2017. Mutual information and error probability analysis on generalized spatial modulation system. *IEEE Trans Commun*, 65(3):1044-1060. <https://doi.org/10.1109/TCOMM.2016.2635127>
- Beth RA, 1936. Mechanical detection and measurement of the angular momentum of light. *Phys Rev*, 50(2):115-125. <https://doi.org/10.1103/PhysRev.50.115>
- Cover TM, Thomas JA, 2006. Elements of Information Theory (2nd Ed.). Wiley-Interscience, Hoboken, USA.
- Edfors O, Johansson AJ, 2012. Is orbital angular momentum (OAM) based radio communication an unexploited area? *IEEE Trans Antenn Propag*, 60(2):1126-1131. <https://doi.org/10.1109/TAP.2011.2173142>
- Gallager RG, 1968. Information Theory and Reliable Communication. Wiley, New York, USA.
- Ge XH, Zi R, Xiong XS, et al., 2017. Millimeter wave communications with OAM-SM scheme for future mobile networks. *IEEE J Sel Areas Commun*, 35(9):2163-2177. <https://doi.org/10.1109/JSAC.2017.2720238>
- Gibson G, Courtial J, Padgett MJ, et al., 2004. Free-space information transfer using light beams carrying orbital angular momentum. *Opt Expr*, 12(22):5448-5456. <https://doi.org/10.1364/OPEX.12.005448>
- Goldsmith A, Jafar SA, Jindal N, et al., 2003. Capacity limits of MIMO channels. *IEEE J Sel Areas Commun*, 21(5): 684-702. <https://doi.org/10.1109/JSAC.2003.810294>
- GSMR, 2011. Mobile Industry Observatory. GSMR, London, UK.
- Hui XN, Zheng SL, Chen YL, et al., 2015. Multiplexed millimeter wave communication with dual orbital angular momentum (OAM) mode antennas. *Sci Rep*, 5:10148. <https://doi.org/10.1038/srep10148>
- Irshid MI, Salous IS, 1991. Bit error probability for coherent M-ary PSK systems. *IEEE Trans Commun*, 39(3):349-352. <https://doi.org/10.1109/26.79269>
- Liu P, di Renzo M, Springer A, 2016. Line-of-sight spatial modulation for indoor mmWave communication at 60 GHz. *IEEE Trans Wirel Commun*, 15(11):7373-7389. <https://doi.org/10.1109/TWC.2016.2601616>
- Mesleh R, Haas H, Ahn CW, et al., 2006. Spatial modulation: a new low complexity spectral efficiency enhancing technique. Proc 1st Int Conf on Communication and Networking in China, p.1-5. <https://doi.org/10.1109/CHINACOM.2006.344658>
- Mohammadi SM, Daldorff LKS, Forozesh K, et al., 2010. Orbital angular momentum in radio: measurement methods. *Radio Sci*, 45(4):RS4007. <https://doi.org/10.1029/2009RS004299>
- Mood AM, Graybill FA, Boes DC, 1974. Introduction to the Theory of Statistics (3rd Ed.). McGraw-Hill, New York, USA.
- Rappaport TS, 1996. Wireless Communications: Principles and Practice. Prentice Hall PTR, Upper Saddle River, USA.
- Schemmel P, Maccalli S, Pisano G, et al., 2014. Three-dimensional measurements of a millimeter wave orbital angular momentum vortex. *Opt Lett*, 39(3):626. <https://doi.org/10.1364/OL.39.000626>
- Simon MK, Alouini MS, 2005. Digital Communication over Fading Channels (2nd Ed.). John Wiley & Sons, New York, USA.
- Stavridis A, Sinanovi S, di Renzo M, et al., 2012. An energy saving base station employing spatial modulation. Proc IEEE 17th Int Workshop on Computer Aided Modeling and Design of Communication Links and Networks, p.231-235. <https://doi.org/10.1109/CAMAD.2012.6335340>
- Tamburini F, Mari E, Sponselli A, et al., 2012. Encoding many channels on the same frequency through radio vorticity: first experimental test. *New J Phys*, 14:033001. <https://doi.org/10.1088/1367-2630/14/3/033001>
- Thidé B, Then H, Sjöholm J, et al., 2007. Utilization of photon orbital angular momentum in the low-frequency radio domain. *Phys Rev Lett*, 99(8):087701. <https://doi.org/10.1103/PhysRevLett.99.087701>
- Wang J, Yang JY, Fazal IM, et al., 2012. Terabit free-space data transmission employing orbital angular momentum multiplexing. *Nat Photon*, 6(7):488-496. <https://doi.org/10.1038/nphoton.2012.138>
- Wang L, Ge XH, Zi R, et al., 2017. Capacity analysis of orbital angular momentum wireless channels. *IEEE Access*, 5:23069-23077. <https://doi.org/10.1109/ACCESS.2017.2763679>
- Willner AE, Wang J, Huang H, 2012. A different angle on light communications. *Science*, 337(6095):655-656. <https://doi.org/10.1126/science.1225460>

- Xiao Y, Yang ZF, Dan LL, et al., 2014. Low-complexity signal detection for generalized spatial modulation. *IEEE Commun Lett*, 18(3):403-406.
https://doi.org/10.1109/LCOMM.2013.123113.132586
- Yan Y, Xie GD, Lavery MPJ, et al., 2014. High-capacity millimetre-wave communications with orbital angular momentum multiplexing. *Nat Commun*, 5(1):4876.
https://doi.org/10.1038/ncomms5876
- Yao AM, Padgett MJ, 2011. Orbital angular momentum: origins, behavior and applications. *Adv Opt Photon*, 3(2): 161-204. https://doi.org/10.1364/AOP.3.000161
- Younis A, Serafimovski N, Mesleh R, et al., 2010. Generalised spatial modulation. Conf Record of the 44th Asilomar Conf on Signals, Systems and Computers, p.1498-1502. https://doi.org/10.1109/ACSSC.2010.5757786
- Zhang R, Yang LL, Hanzo L, 2015. Error probability and capacity analysis of generalised pre-coding aided spatial modulation. *IEEE Trans Wirel Commun*, 14(1):364-375. https://doi.org/10.1109/TWC.2014.2347297
- Zhang WT, Zheng SL, Hui XN, et al., 2017. Mode division multiplexing communication using microwave orbital angular momentum: an experimental study. *IEEE Trans Wirel Commun*, 16(2):1308-1318.
https://doi.org/10.1109/TWC.2016.2645199
- Zhang ZF, Zheng SL, Chen YL, et al., 2016. The capacity gain of orbital angular momentum based multiple-input-multiple-output system. *Sci Rep*, 6:25418.
https://doi.org/10.1038/srep25418
- Zheng SL, Hui XN, Jin XF, et al., 2015a. Generation of OAM millimeter waves using traveling-wave circular slot antenna based on ring resonant cavity. IEEE Int Conf on Computational Electromagnetics, p.239-240.
https://doi.org/10.1109/COMPEN.2015.7052619
- Zheng SL, Hui XN, Jin XF, et al., 2015b. Transmission characteristics of a twisted radio wave based on circular traveling-wave antenna. *IEEE Trans Antenn Propag*, 63(4):1530-1536.
https://doi.org/10.1109/TAP.2015.2393885

Appendix A: Proof of Theorem 1

We consider that all elements in \mathbf{W} in the input and output equations of the system are additive white Gaussian noise with a mean of 0 and variance of σ_w^2 , and that symbol vector \mathbf{s}_i , antenna selection matrix \mathbf{A}_i , and channel matrix \mathbf{H}_k are known. Thus, the conditional probability density function (PDF) of the signal vector \mathbf{y} received by a receiver can be expressed as

$$p(\mathbf{y}|\mathbf{H}_k, \mathbf{A}_i, \mathbf{s}_j) = \frac{1}{\pi\sigma_w^2} \exp\left(-\frac{1}{\sigma_w^2} \|\mathbf{y} - \mathbf{H}_k \mathbf{A}_i \mathbf{s}_j\|^2\right), \quad (\text{A1})$$

where $p(\cdot)$ represents the PDF of random variables.

When discrete input is uniformly distributed, channel capacity reaches the maximum (Goldsmith et al., 2003). As can be seen from the above, the selection of activated antenna matrix \mathbf{A}_i , modulation symbol vector \mathbf{s}_j , and channel gain matrix \mathbf{H}_k depends on an input random bit stream. Assuming that each bit of the input is independent and uniformly distributed, \mathbf{A}_i , \mathbf{s}_j , and \mathbf{H}_k are selected from activated antenna matrix set \mathbb{A} , modulation symbol vector signal set \mathbb{S} , and all possible channel gain matrix set \mathbb{H} with a medium probability, respectively. Thus, channel capacity reaches the maximum value when all are equally probabilistic. Thus, we have

$$p(\mathbf{A}_i) = 1/\mathcal{N}, \quad (\text{A2})$$

$$p(\mathbf{s}_j) = 1/\mathcal{S}, \quad (\text{A3})$$

$$p(\mathbf{H}_k) = 1/\mathcal{L}. \quad (\text{A4})$$

According to the conditional probability expression in Eq. (A1), the PDF of the received symbol vector \mathbf{y} can be obtained as follows:

$$\begin{aligned} p(\mathbf{y}) &= \sum_{k=1}^{\mathcal{L}} \sum_{j=1}^{\mathcal{S}} \sum_{i=1}^{\mathcal{N}} p(\mathbf{y}, \mathbf{H}_k, \mathbf{A}_i, \mathbf{s}_j) \\ &= \frac{1}{\mathcal{L}\mathcal{S}\mathcal{N}} \sum_{k=1}^{\mathcal{L}} \sum_{j=1}^{\mathcal{S}} \sum_{i=1}^{\mathcal{N}} p(\mathbf{y}|\mathbf{H}_k, \mathbf{A}_i, \mathbf{s}_j) \\ &= \frac{1}{\mathcal{L}\mathcal{S}\mathcal{N}\pi\sigma_w^2} \sum_{k=1}^{\mathcal{L}} \sum_{j=1}^{\mathcal{S}} \sum_{i=1}^{\mathcal{N}} \exp\left(-\frac{\|\mathbf{y} - \mathbf{H}_k \mathbf{A}_i \mathbf{s}_j\|^2}{\sigma_w^2}\right). \end{aligned} \quad (\text{A5})$$

Through Eq. (A1), we can obtain that for the case where the antenna selection matrix is \mathbf{A}_i , modulation symbol vector is \mathbf{s}_i , channel gain matrix is \mathbf{H}_k , and receiving symbol vector is \mathbf{y} , the PDF can be expressed as

$$\begin{aligned} p(\mathbf{y}, \mathbf{H}_k, \mathbf{A}_i, \mathbf{s}_j) &= \frac{1}{\mathcal{L}\mathcal{S}\mathcal{N}\pi\sigma_w^2} \exp\left(-\frac{\|\mathbf{y} - \mathbf{H}_k \mathbf{A}_i \mathbf{s}_j\|^2}{\sigma_w^2}\right) \\ &= \frac{1}{\mathcal{L}\mathcal{S}\mathcal{N}\pi\sigma_w^2} \exp\left(-\frac{\|\mathbf{W}\|^2}{\sigma_w^2}\right). \end{aligned} \quad (\text{A6})$$

Substituting Eqs. (A5) and (A6) into channel capacity Eq. (12b), Eq. (12b) can be further derived as

$$\begin{aligned}
\delta &= \log_2 \frac{p(\mathbf{y} | \mathbf{H}_k, \mathbf{A}_i, \mathbf{s}_j)}{\sum_{k_1=1}^{\mathcal{L}} \sum_{j_1=1}^{\mathcal{S}} \sum_{i_1=1}^{\mathcal{N}} p(\mathbf{y}, \mathbf{H}_{k_1}, \mathbf{A}_{i_1}, \mathbf{s}_{j_1})} \\
&= \log_2 \frac{\frac{1}{\pi \sigma_w^2} \exp\left(-\frac{\|\mathbf{y} - \mathbf{H}_k \mathbf{A}_i \mathbf{s}_j\|^2}{\sigma_w^2}\right)}{\frac{1}{\mathcal{L} \mathcal{S} \mathcal{N} \pi \sigma_w^2} \sum_{k_1=1}^{\mathcal{L}} \sum_{j_1=1}^{\mathcal{S}} \sum_{i_1=1}^{\mathcal{N}} \exp\left(-\frac{\|\mathbf{y} - \mathbf{H}_{k_1} \mathbf{A}_{i_1} \mathbf{s}_{j_1}\|^2}{\sigma_w^2}\right)} \\
&= \log_2 \mathcal{L} \mathcal{S} \mathcal{N} - \log_2 \left(\exp\left(\frac{-\|\mathbf{W}\|^2}{\sigma_w^2}\right)^{-1} \cdot \sum_{k_1=1}^{\mathcal{L}} \sum_{j_1=1}^{\mathcal{S}} \sum_{i_1=1}^{\mathcal{N}} \exp\left(\frac{-\|\mathbf{y} - \mathbf{H}_{k_1} \mathbf{A}_{i_1} \mathbf{s}_{j_1}\|^2}{\sigma_w^2}\right) \right) \\
&= \log_2 \mathcal{L} \mathcal{S} \mathcal{N} - \log_2 \sum_{k_1=1}^{\mathcal{L}} \sum_{j_1=1}^{\mathcal{S}} \sum_{i_1=1}^{\mathcal{N}} \exp\left(\frac{1}{\sigma_w^2} \left(\|\mathbf{W}\|^2 - \|\mathbf{H}_{k_1} \mathbf{A}_{i_1} \mathbf{s}_{j_1} - \mathbf{H}_{k_1} \mathbf{A}_{i_1} \mathbf{s}_{j_1} + \mathbf{W}\|^2 \right)\right). \tag{A7}
\end{aligned}$$

The channel capacity formula can be derived as

$$\begin{aligned}
C &= \max_{p(\mathbf{s}_j), p(\mathbf{A}_i), p(\mathbf{H}_k)} \sum_{k=1}^{\mathcal{L}} \sum_{j=1}^{\mathcal{S}} \sum_{i=1}^{\mathcal{N}} \int_{-\infty}^{\infty} p(\mathbf{y}, \mathbf{H}_k, \mathbf{A}_i, \mathbf{s}_j) \\
&\quad \cdot \log_2 \frac{p(\mathbf{y} | \mathbf{H}_k, \mathbf{A}_i, \mathbf{s}_j)}{\sum_{k_1=1}^{\mathcal{L}} \sum_{j_1=1}^{\mathcal{S}} \sum_{i_1=1}^{\mathcal{N}} p(\mathbf{y}, \mathbf{H}_{k_1}, \mathbf{A}_{i_1}, \mathbf{s}_{j_1})} \mathrm{d}\mathbf{y} \\
&= \sum_{k=1}^{\mathcal{L}} \sum_{j=1}^{\mathcal{S}} \sum_{i=1}^{\mathcal{N}} \int_{-\infty}^{\infty} \frac{1}{\mathcal{L} \mathcal{S} \mathcal{N} \pi \sigma_w^2} \exp\left(\frac{-\|\mathbf{W}\|^2}{\sigma_w^2}\right) \left(\log_2 \mathcal{L} \mathcal{S} \mathcal{N} \right. \\
&\quad \left. - \log_2 \sum_{k_1=1}^{\mathcal{L}} \sum_{j_1=1}^{\mathcal{S}} \sum_{i_1=1}^{\mathcal{N}} \exp\left(\frac{\|\mathbf{W}\|^2 - \|\mathbf{y} - \mathbf{H}_{k_1} \mathbf{A}_{i_1} \mathbf{s}_{j_1}\|^2}{\sigma_w^2}\right) \right) \mathrm{d}\mathbf{y} \\
&= \log_2 \mathcal{L} \mathcal{S} \mathcal{N} - \sum_{k=1}^{\mathcal{L}} \sum_{j=1}^{\mathcal{S}} \sum_{i=1}^{\mathcal{N}} \mathbb{E}(\mathbf{W}) \left(\log_2 \sum_{k_1=1}^{\mathcal{L}} \sum_{j_1=1}^{\mathcal{S}} \sum_{i_1=1}^{\mathcal{N}} e^{\psi} \right), \tag{A8a}
\end{aligned}$$

$$\psi = \frac{1}{\sigma_w^2} \left(\|\mathbf{W}\|^2 - \|\mathbf{H}_k \mathbf{A}_i \mathbf{s}_j - \mathbf{H}_{k_1} \mathbf{A}_{i_1} \mathbf{s}_{j_1} + \mathbf{W}\|^2 \right). \tag{A8b}$$

Appendix B: Proof of Theorem 2

When detecting the activated antenna combination, the combination with the largest sum of signal strengths in the receiving antenna is determined as the selected active mode. Since each pair of receiving antennas at the receiver is arranged in the intensity focusing circular area where the intensity of the OAM beam is the greatest, each pair of receiving antennas needs only to compare the signal strength received by one of the antennas. Here, each pair of receiving antennas takes the signal obtained by the first antenna. From the analysis of the system model, it can be concluded that the signal received by antenna $\text{RX}_{j,1}$ can be expressed as

$$y_{j,1} = \sqrt{\rho} \sum_{i=1}^{M_a} h_{JC(k,i),1}^{LC(k,i)} s_i + \omega, \tag{B1}$$

where the noise is $\omega \sim \mathcal{CN}(0, \sigma_w^2)$, ρ is the transmission power of the OAM-GSM communication system, and \mathbf{s}_i is the i^{th} vector in vector signal set \mathbb{S} . As shown in Eqs. (B2) and (B3), the signal strength at receiving antenna $\text{RX}_{v_i,1}$ corresponding to an active transmitting antenna can be represented by $|y_{v_i,1}|^2$, and the signal strength at receiving antenna $\text{RX}_{u_i,1}$ corresponding to an inactive transmitting antenna can be expressed by $|y_{u_i,1}|^2$. $\sigma_0^2 = \sigma_w^2/2$. $\Re(\cdot)$ and $\Im(\cdot)$ represent taking the real part and imaginary part, respectively.

$$\begin{aligned}
|y_{v_i,1}|^2 &= \mathbb{R}(y_{v_i,1})^2 + \mathbb{I}(y_{v_i,1})^2 \\
&\sim \mathcal{N} \left(\mathbb{R} \left(\sqrt{\rho} \left\{ \sum_{i=1}^{M_a} h_{v_i C(k,i),1}^{LC(k,i)} s_i \right\} \right), \sigma_0^2 \right) \\
&+ \mathcal{N} \left(\mathbb{I} \left(\sqrt{\rho} \left\{ \sum_{i=1}^{M_a} h_{v_i C(k,i),1}^{LC(k,i)} s_i \right\} \right), \sigma_0^2 \right) \quad \forall v_i \in C(k), \tag{B2}
\end{aligned}$$

$$\begin{aligned}
 |y_{u_i,1}|^2 &= \mathbb{R}(y_{u_i,1})^2 + \mathbb{I}(y_{u_i,1})^2 \\
 &\sim \mathcal{N}\left(\mathbb{R}\left(\sqrt{\rho}\left\{\sum_{i=1}^{M_a} h_{u_i C(k,i)}^{l_{C(k,i)}} \mathbf{s}_i\right\}\right), \sigma_0^2\right) \\
 &+ \mathcal{N}\left(\mathbb{I}\left(\sqrt{\rho}\left\{\sum_{i=1}^{M_a} h_{u_i C(k,i)}^{l_{C(k,i)}} \mathbf{s}_i\right\}\right), \sigma_0^2\right) \quad \forall u_i \in \bar{C}(k).
 \end{aligned} \tag{B3}$$

Based on the definition of chi-square distribution (Mood et al., 1974), Eqs. (B2) and (B3) can be written as

$$|y_{v_i,1}|^2 \sim \chi_2^2(g; \lambda_{v_i,1}), \tag{B4}$$

$$|y_{u_i,1}|^2 \sim \chi_2^2(g; \lambda_{u_i,1}), \tag{B5}$$

where $\chi_2^2(g; \lambda_{v_i,1})$ is the non-central chi-square distribution of g and the degree of freedom is 2. In

Eq. (B4), $\lambda_{v_i,1} = \rho \left| \sum_{i=1}^{M_a} h_{v_i C(k,i)}^{l_{C(k,i)}} \mathbf{s}_i \right|^2 / \sigma_0^2$. In Eq. (B5),

$\lambda_{u_i,1} = \rho \left| \sum_{i=1}^{M_a} h_{u_i C(k,i)}^{l_{C(k,i)}} \mathbf{s}_i \right|^2 / \sigma_0^2$. \mathbf{s}_i is the symbol vector

adopted by the corresponding transmitting antenna. According to the power intensity of the received signal, the probability of correctly judging the transmitting antenna index is given by

$$\begin{aligned}
 &P(\Theta_{\text{ant}}) \\
 &= \int_0^\infty P(|y_{u_1,1}|^2 < g_{v_1,1}, \dots, |y_{u_{M-M_a},1}|^2 < g_{v_1,1}, \\
 &\quad \dots, |y_{u_1,1}|^2 < g_{v_{M_a},1}, \dots, |y_{u_{M-M_a},1}|^2 < g_{v_{M_a},1}) \\
 &\quad \cdot P(|y_{v_1,1}|^2 = g_{v_1,1}, \dots, |y_{v_{M_a},1}|^2 = \\
 &\quad g_{v_{M_a},1} | \lambda_{v_1,1}, \dots, \lambda_{v_{M_a},1}) \mathbf{d}g_{v_1,1} \dots \mathbf{d}g_{v_{M_a},1} \\
 &= \prod_{i=1}^{M_a} \int_0^\infty P(|y_{u_i,1}|^2 < g_{v_i,1}, \dots, |y_{u_{M-M_a},1}|^2 < g_{v_i,1}) \\
 &\quad \cdot P(|y_{v_i,1}|^2 = g_{v_i,1} | \lambda_{v_i,1}) \mathbf{d}g_{v_i,1} \\
 &= \prod_{i=1}^{M_a} \int_0^\infty \prod_{u_j \in \bar{C}(k)} P(|y_{u_j,1}|^2 < g_{v_i,1}) \\
 &\quad \cdot P(|y_{v_i,1}|^2 = g_{v_i,1} | \lambda_{v_i,1}) \mathbf{d}g_{v_i,1} \\
 &= \prod_{i=1}^{M_a} \int_0^\infty \prod_{u_j \in \bar{C}(k)} F_{\chi_2^2}(g; \lambda_{u_j,1}) f_{\chi_2^2}(g; \lambda_{v_i,1}) \mathbf{d}g,
 \end{aligned} \tag{B6}$$

where Θ_{ant} is the event of correctly detecting the activated antenna matrix (Zhang R et al., 2015).

$P(|y_{v_i,1}|^2 = g_{v_i,1} | \lambda_{v_i,1})$ represents the probability that the signal strength received by the activated antenna is equal to $g_{v_i,1}$ and $P(|y_{u_1,1}|^2 < g_{v_1,1}, \dots, |y_{u_{M-M_a},1}|^2 < g_{v_i,1})$ represents the probability that the signal strength received by other antennas is smaller than $g_{v_i,1}$. $F_{\chi_2^2}(g; \lambda_{u_j,1})$ is the cumulative distribution function of the chi-square distribution, and $f_{\chi_2^2}(g; \lambda_{v_i,1})$ is the PDF of the chi-square distribution.

The SER of the space signal part is

$$\begin{aligned}
 e_{\text{ant}}^s &= 1 - \frac{1}{2^{k_{\text{ant}}}} \sum_{k=1}^{2^{k_{\text{ant}}}} \prod_{i=1}^{M_a} \int_0^\infty \prod_{u_j \in \bar{C}(k)} F_{\chi_2^2}(g; \lambda_{u_j,1}) \\
 &\quad \cdot f_{\chi_2^2}(g; \lambda_{v_i,1}) \mathbf{d}g.
 \end{aligned} \tag{B7}$$

When azimuth σ is reasonably set, the judgment of the OAM state must be correct, so the SER of the OAM state signal is $e_{\text{OAM}}^s = 0$ (Ge et al., 2017). The SER of the P -point constellation modulation symbol is (Irshid and Salous, 1991; Simon and Alouini, 2005)

$$\begin{aligned}
 e_{\text{mod}}^s &= \frac{1}{P^{M_a}} \\
 &\cdot \sum_{p=1}^{P^{M_a}} \sum_{p_1=1}^{P^{M_a}} \left[\mathbb{D}(\mathbf{s}_p, \mathbf{s}_{p_1}) \cdot \mathbb{Q}\left(\sqrt{\frac{\rho}{2\sigma_w^2}} \|\mathbf{H}_1 \mathbf{A}(\mathbf{s}_p - \mathbf{s}_{p_1})\|\right) \right],
 \end{aligned} \tag{B8}$$

where \mathbf{s}_p is the symbol vector received by the receiver, \mathbf{s}_{p_1} is the symbol vector demodulated, $\mathbb{D}(\mathbf{s}_p, \mathbf{s}_{p_1})$ represents the Hamming distance between \mathbf{s}_p and \mathbf{s}_{p_1} , and $\mathbb{Q}(\cdot)$ is a Q-function.

When considering whether the activated antenna is detected correctly, the SER of the modulation symbol is (Zhang R et al., 2015)

$$\tilde{e}_{\text{mod}}^s = (1 - e_{\text{ant}}^s) e_{\text{mod}}^s + e_{\text{ant}}^s \sum_{l \neq k} \frac{M_c e_{\text{mod}}^s + M_d e_0^s}{M_a (2^{k_{\text{ant}}} - 1)}, \tag{B9}$$

where M_d is the number of different antennas between detection activated antennas and actual activated antennas, and M_c is the number of the same antennas between detection activated antennas and actual activated antennas. $e_0^s = (P - 1) / P$ is the SER of the modulation symbol detected when the corresponding transmitting antenna is an inactivated antenna due to an error in activating antenna judgment.

When considering whether the activated antennas are detected correctly, the SER of the OAM state symbol is

$$\tilde{e}_{\text{OAM}}^s = e_{\text{ant}}^s \sum_{l \neq k} \frac{M_d}{M_a (2^{k_{\text{ant}}} - 1)}. \quad (\text{B10})$$

The relationship between BER and SER can be approximated as

$$e_{\text{ant}}^b = \delta_{k_{\text{ant}}} e_{\text{ant}}^s / k_{\text{ant}}, \quad (\text{B11})$$

$$\tilde{e}_{\text{mod}}^b = \tilde{e}_{\text{mod}}^s / k_{\text{mod}}, \quad (\text{B12})$$

$$\tilde{e}_{\text{OAM}}^b = \tilde{e}_{\text{OAM}}^s / k_{\text{OAM}}, \quad (\text{B13})$$

where $\delta_{k_{\text{ant}}} = \delta_{k_{\text{ant}-1}} + (2^{\delta_{k_{\text{ant}-1}}} - \delta_{k_{\text{ant}-1}}) / (2^{\delta_{k_{\text{ant}}}} - 1)$, $\delta_0 = 0$.

Therefore, the BER of the OAM-GSM system can be expressed as

$$e^b = \frac{k_{\text{ant}} e_{\text{ant}}^b + M_a k_{\text{mod}} \tilde{e}_{\text{mod}}^b + M_a k_{\text{OAM}} \tilde{e}_{\text{OAM}}^b}{k_{\text{ant}} + M_a k_{\text{mod}} + M_a k_{\text{OAM}}} = \frac{\delta_{k_{\text{ant}}} e_{\text{ant}}^s + M_a \tilde{e}_{\text{mod}}^s + M_a \tilde{e}_{\text{OAM}}^s}{k_{\text{ant}} + M_a k_{\text{mod}} + M_a k_{\text{OAM}}}. \quad (\text{B14})$$

Appendix C: Proof of Theorem 3

After the precoding module is added, when detecting a combination of the activated antenna, the signal at the receiving antenna $\text{RX}_{v_i,1}$ corresponding to an active transmitting antenna can be represented by $\dot{y}_{v_i,1}$, and the signal at the receiving antenna $\text{RX}_{u_i,1}$ corresponding to an inactive transmitting antenna can be represented by $\dot{y}_{u_i,1}$:

$$\dot{y}_{v_i,1} = \sqrt{\rho} x_i + \omega \quad \forall v_i \in C(k), \quad (\text{C1})$$

$$\dot{y}_{u_i,1} = \omega \quad \forall u_i \in \bar{C}(k), \quad (\text{C2})$$

where x_i represents the signal emitted by the i^{th} activated antenna. The signal strengths received by receiving antennas $\text{RX}_{v_i,1}$ and $\text{RX}_{u_i,1}$ are

$$|\dot{y}_{v_i,1}|^2 = \mathbb{R}(\dot{y}_{v_i,1})^2 + \mathbb{I}(\dot{y}_{v_i,1})^2 \sim \mathcal{N}(\mathbb{R}(\sqrt{\rho} x_i), \sigma_0^2) + \mathcal{N}(\mathbb{I}(\sqrt{\rho} x_i), \sigma_0^2), \quad (\text{C3})$$

$$|\dot{y}_{u_i,1}|^2 = \mathbb{R}(\dot{y}_{u_i,1})^2 + \mathbb{I}(\dot{y}_{u_i,1})^2 \sim \mathcal{N}(0, \sigma_0^2) + \mathcal{N}(0, \sigma_0^2). \quad (\text{C4})$$

Based on the definition of the chi-square distribution, the above formulae can be written as

$$|\dot{y}_{v_i,1}|^2 \sim \chi_2^2(g; \dot{\lambda}_{v_i,1}), \quad (\text{C5})$$

$$|\dot{y}_{u_i,1}|^2 \sim \chi_2^2(g), \quad (\text{C6})$$

where $\chi_2^2(g; \dot{\lambda}_{v_i,1})$ is the non-central chi-square distribution of random variable g (the degree of freedom is 2), $\dot{\lambda}_{v_i,1} = \rho |s_i|^2 / \sigma_0^2$, and $\chi_2^2(g)$ is the chi-square distribution of g (the degree of freedom is 2).

In the system with added precoding, the probability of correctly judging the transmitting antenna index is given by

$$\begin{aligned} & \dot{P}(\Theta_{\text{ant}}) \\ &= \int_0^\infty P(|\dot{y}_{u_1,1}|^2 < g_{v_1,1}, \dots, |\dot{y}_{u_{M-M_a},1}|^2 < g_{v_1,1}, \\ & \quad \dots, |\dot{y}_{u_1,1}|^2 < g_{v_{M_a},1}, \dots, |\dot{y}_{u_{M-M_a},1}|^2 < g_{v_{M_a},1}) \\ & \cdot P(|\dot{y}_{v_1,1}|^2 = g_{v_1,1}, \dots, |\dot{y}_{v_{M_a},1}|^2 = g_{v_{M_a},1} | \dot{\lambda}_{v_1,1}, \dots, \dot{\lambda}_{v_{M_a},1}) \\ & \text{d}g_{v_1,1} \dots \text{d}g_{v_{M_a},1} \\ &= \prod_{i=1}^{M_a} \int_0^\infty P(|\dot{y}_{u_1,1}|^2 < g_{v_i,1}, \dots, |\dot{y}_{u_{M-M_a},1}|^2 < g_{v_i,1}) \\ & \quad \cdot P(|\dot{y}_{v_i,1}|^2 = g_{v_i,1} | \dot{\lambda}_{v_i,1}) \text{d}g_{v_i,1} \\ &= \prod_{i=1}^{M_a} \int_0^\infty \prod_{u_j \in \bar{C}(k)} P(|\dot{y}_{u_j,1}|^2 < g_{v_i,1}) \\ & \quad \cdot P(|\dot{y}_{v_i,1}|^2 = g_{v_i,1} | \dot{\lambda}_{v_i,1}) \text{d}g_{v_i,1} \\ &= \prod_{i=1}^{M_a} \int_0^\infty [F_{\chi_2^2}(g)]^{M-M_a} f_{\chi_2^2}(g; \dot{\lambda}_{v_i,1}) \text{d}g, \end{aligned} \quad (\text{C7})$$

where $P(|\dot{y}_{v_i,1}|^2 = g_{v_i,1} | \dot{\lambda}_{v_i,1})$ represents the probability that the signal strength received by the activated antenna is equal to $g_{v_i,1}$, $(|\dot{y}_{u_1,1}|^2 < g_{v_i,1}, \dots, |\dot{y}_{u_{M-M_a},1}|^2 < g_{v_i,1})$ represents the probability that the signal strength received by other antennas is less than $g_{v_i,1}$, $F_{\chi^2_2}(g)$ is the cumulative distribution function of the chi-square distribution and $f_{\chi^2_2}(g; \dot{\lambda}_{v_i,1})$ is the PDF of the chi-square distribution. Thus, the SER of the spatial signal part of the system after adding the precoding module is

$$\dot{e}_{\text{ant}}^s = 1 - \frac{1}{2^{k_{\text{ant}}}} \sum_{k=1}^{2^{k_{\text{ant}}}} \prod_{i=1}^{M_a} \int_0^\infty [F_{\chi^2_2}(g)]^{M-M_a} f_{\chi^2_2}(g; \dot{\lambda}_{v_i,1}) dg. \tag{C8}$$

After adding the precoding module, the SER of the system's P -point constellation modulation symbol is

$$\dot{e}_{\text{mod}}^s = \frac{1}{P} \sum_{p=1}^P \sum_{p_1=1}^P \left[\mathbb{D}(\mathbf{s}_p, \mathbf{s}_{p_1}) \cdot \mathbb{Q} \left(\sqrt{\frac{\rho}{2\sigma_w^2}} |\mathbf{s}_p - \mathbf{s}_{p_1}| \right) \right]. \tag{C9}$$

When azimuth σ is reasonably set, the judgment of the OAM state must be correct, so the SER of the OAM state signal is $\dot{e}_{\text{OAM}}^s = 0$.

Considering whether the activated antenna is detected correctly, the SER of the system's modulation symbol after adding the precoding module is

$$\dot{e}_{\text{mod}}^s = (1 - \dot{e}_{\text{ant}}^s) \dot{e}_{\text{mod}}^s + \dot{e}_{\text{ant}}^s \sum_{l \neq k} \frac{M_c \dot{e}_{\text{mod}}^s + M_d e_0^s}{M_a (2^{k_{\text{ant}}} - 1)}. \tag{C10}$$

Considering whether the activated antennas are detected correctly, the SER of the system's OAM state symbol after adding the precoding module is

$$\dot{e}_{\text{OAM}}^s = \dot{e}_{\text{ant}}^s \sum_{l \neq k} \frac{M_d}{M_a (2^{k_{\text{ant}}} - 1)}. \tag{C11}$$

The relationship between BER and SER can be approximated as

$$\dot{e}_{\text{ant}}^b \approx \delta_{k_{\text{ant}}} \dot{e}_{\text{ant}}^s / k_{\text{ant}}, \tag{C12}$$

$$\dot{e}_{\text{mod}}^b \approx \dot{e}_{\text{mod}}^s / k_{\text{mod}}, \tag{C13}$$

$$\dot{e}_{\text{OAM}}^b \approx \dot{e}_{\text{OAM}}^s / k_{\text{OAM}}, \tag{C14}$$

where $\delta_{k_{\text{ant}}} = \delta_{k_{\text{ant}}-1} + (2^{\delta_{k_{\text{ant}}-1}} - \delta_{k_{\text{ant}}-1}) / (2^{\delta_{k_{\text{ant}}}} - 1)$, $\delta_0=0$.

Therefore, the total BER of the system after adding the precoding module can be expressed as

$$\begin{aligned} \dot{e}^b &= \frac{k_{\text{ant}} \dot{e}_{\text{ant}}^b + M_a k_{\text{mod}} \dot{e}_{\text{mod}}^b + M_a k_{\text{OAM}} \dot{e}_{\text{OAM}}^b}{k_{\text{ant}} + M_a k_{\text{mod}} + M_a k_{\text{OAM}}} \\ &= \frac{\delta_{k_{\text{ant}}} \dot{e}_{\text{ant}}^s + M_a \dot{e}_{\text{mod}}^s + M_a \dot{e}_{\text{OAM}}^s}{k_{\text{ant}} + M_a k_{\text{mod}} + M_a k_{\text{OAM}}}. \end{aligned} \tag{C15}$$